

000 001 002 003 004 005 006 007 008 009 010 011 012 013 014 015 016 017 018 019 020 021 022 023 024 025 026 027 028 029 030 031 032 033 034 035 036 037 038 039 040 041 042 043 044 045 046 047 048 049 050 051 052 053 054 055 056 057 FROM WHAT TO WHY: A MULTI-AGENT SYSTEM FOR EVIDENCE-BASED CHEMICAL REACTION CONDITION REA- SONING

006 **Anonymous authors**

007 Paper under double-blind review

ABSTRACT

013 The chemical reaction recommendation is to select proper reaction condition parameters for
014 chemical reactions, which is pivotal to accelerating chemical science. With the rapid develop-
015 ment of large language models (LLMs), there is growing interest in leveraging their reasoning
016 and planning capabilities for reaction condition recommendation. Despite their success, existing
017 methods rarely explain the rationale behind the recommended reaction conditions, limiting their
018 utility in high-stakes scientific workflows. In this work, we propose ChemMAS, a multi-agent
019 system that reframes condition prediction as an evidence-based reasoning task. ChemMAS
020 decomposes the task into mechanistic grounding, multi-channel recall, constraint-aware agen-
021 tic debate, and rationale aggregation. Each decision is backed by interpretable justifications
022 grounded in chemical knowledge and retrieved precedents. Experiments show that ChemMAS
023 achieves 20–35% gains over domain-specific baselines and outperforms general-purpose LLMs
024 by 10–15% in Top-1 similarity, while offering falsifiable, human-trustable rationales, which
025 establishes a new paradigm for explainable AI in scientific discovery.

1 INTRODUCTION

028 The progress in chemistry has long relied on the ability to design chemically valid reactions that yield scientific
029 insights (Tu et al., 2023; Ismail et al., 2022). Central to this task is selecting proper reaction condition parameters,
030 such as solvent, temperature, catalysts, and reagent ratios, which are pivotal to reaction success, selectivity, and
031 scalability (Ball et al., 2025; Taylor et al., 2023). The traditional approach involves extensive human labor to
032 explore the chemical reaction space, which cannot satisfy the growing demand for efficient and safe chemical
033 synthesis (Lyall-Brookes et al., 2025; Ali et al., 2024; Lee et al., 2025). Recent advances in deep learning and data-
034 driven modeling have opened up new opportunities for reaction recommendation, enabling automated exploration
035 of reaction space and the discovery of novel, scalable synthetic routes with minimal manual intervention (Ali
036 et al., 2024; Liu et al., 2023). Early work typically trains relatively small-scale models, such as graph neural
037 networks (Wu et al., 2020) and Transformers (Vaswani et al., 2017), from scratch, achieving strong performance
038 when abundant labeled data are available (Wang et al., 2023).

039 With the rapid development of large language models (Naveed et al., 2025; Zhao et al., 2023) (LLMs), there has
040 been a growing interest in leveraging their powerful reasoning and planning abilities for reaction condition rec-
041 ommendation (Bran et al., 2025). Current LLM-based approaches can be broadly categorized into retrieval-based
042 (Zhang et al., 2024b; Chen et al., 2023) and reasoning-based approaches. Retrieval-based approaches search for
043 similar reactions from external databases and transfer their conditions to the query reaction, which is usually en-
044 hanced by learned molecular embeddings or unsupervised chemical priors to improve retrieval quality (Andronov
045 et al., 2023). In contrast, reasoning-based approaches directly prompt or fine-tune LLMs to infer suitable reaction
046 conditions from molecular structures or textual descriptions (Qian et al., 2023; Zhou et al., 2025), and achieve
047 improved zero-shot and few-shot generalization capabilities.

048 However, despite their success in predicting plausible reaction conditions, these approaches rarely address the
049 deeper scientific question of why such conditions are appropriate. In the context of scientific discovery, under-
050 standing why is arguably more critical than merely predicting what. A reliable system should not only propose
051 a solvent or temperature but also provide a mechanistic justification: Which functional group governs the reac-
052 tivity? What prior experimental evidence supports this choice? Which constraints exclude alternative reagents
053 or solvents? Without such explanatory reasoning, models risk being opaque black boxes, limiting their utility in
054 high-stakes scientific workflows.

055 To tackle this challenge, we introduce ChemMAS, a multi-agent system that treats condition selection as a reason-
056 ing task grounded in chemical knowledge, mechanistic constraints, and peer deliberation. ChemMAS decomposes
057 the problem into four collaborative stages. It first grounds chemical reactivity via mechanistic analysis, where a
058 general chemist agent parses SMILES to identify functional groups, balance stoichiometry, and infer plausible by-
059 products. The system then retrieves condition exemplars through multichannel queries over a structured reaction

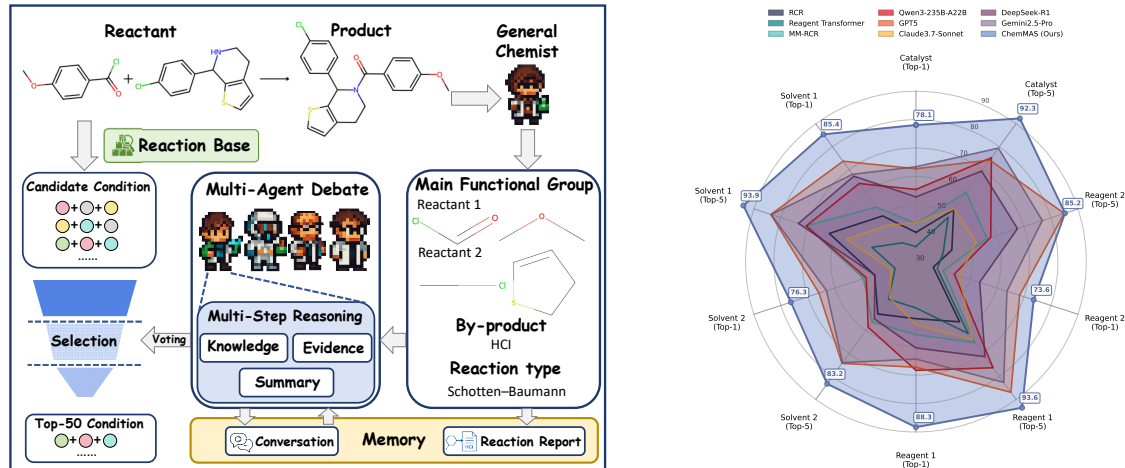


Figure 1: Overview of ChemMAS. A collaborative multi-agent system for evidence-based reaction-condition reasoning from SMILES inputs. ChemMAS demonstrates strong versatility and delivers state-of-the-art performance on reaction condition reasoning.

database. These candidates are refined via a tournament-style elimination process, in which agent panels conduct pairwise comparisons using memory-informed multi-step reasoning. Finally, ChemMAS aggregates rationales for each decision by combining mechanistic plausibility, retrieved evidence, and constraint checks into interpretable justifications.

By shifting from mere top- k ranking to interpretable, evidence-backed reasoning, ChemMAS offers a new paradigm: one that is not only predictive but also justifiable, auditable, and suitable for closed-loop experimentation. In our evaluation, ChemMAS outperforms specialized chemical models (*e.g.*, RCR (Gao et al., 2018), Reagent Transformer (Andronov et al., 2023)) by 20-30% Top-1 similarity and surpasses leading general-purpose LLMs (*e.g.*, GPT-5, Gemini 2.5) by 10-15% on average, validating its effectiveness and robustness.

Our contributions are threefold:

- We reformulate reaction condition recommendation as evidence-based chemical reaction condition reasoning, requiring models to output not only “what”-level conditions but also “why”-level evidence.
- We introduce ChemMAS, a multi-agent system that couples chemistry-aware tool calling with multi-channel recall, multi-step mechanistic reasoning under constraint verification, and debate-based aggregation, producing interpretable, falsifiable condition reasoning.
- We benchmark ChemMAS against specialized chemical models and cutting-edge general-purpose LLMs, showing state-of-the-art performance with up to 30-point gains in Top-1 similarity and robust generalization across diverse condition types.

2 CHEMMAS

2.1 PROBLEM DEFINITION

Unlike the existing reaction condition recommendation, we formalize evidence-based reaction condition reasoning as follows. An input reaction is $\mathbf{x} = (\mathcal{R}, \mathcal{P}, \mathcal{I})$ with reactants \mathcal{R} , products \mathcal{P} , and optional context \mathcal{I} . A condition configuration is a structured object $\mathbf{c} \in \mathcal{C}$, where \mathcal{C} may mix discrete and continuous factors. The system returns K configurations $\widehat{\mathcal{C}} = \{\mathbf{c}_1, \dots, \mathbf{c}_K\}$ and a rationale for each $\rho(\mathbf{c}) = (M, S, E, \Pi)$ comprising domain reasoning M , verifiable checks S , aligned evidence E , and a concise derivation Π . Validity is

$$\text{Valid}(\rho(\mathbf{c}); \mathbf{x}) = \mathbb{1}[\text{Constr}(S) \wedge \text{Align}(E; \mathbf{x}, \mathbf{c}) \geq \delta \wedge \text{Coherent}(\Pi, M, E)]. \quad (1)$$

Here, $\text{Constr}(S)$ is true when all hard checks in S pass. $\text{Align}(E; \mathbf{x}, \mathbf{c}) \in [0, 1]$ scores how well the evidence E supports (\mathbf{x}, \mathbf{c}) using signals such as reaction-type matches, functional-group overlap, MCS alignment, or learned embeddings, with δ as a fixed threshold. $\text{Coherent}(\Pi, M, E)$ verifies that the derivation Π is logically consistent with the mechanistic summary M and the evidence E . The indicator $\mathbb{1}$ returns 1 only when all criteria hold. The objective is

$$\max_{\widehat{\mathcal{C}}, \rho} \sum_{\mathbf{c} \in \widehat{\mathcal{C}}} u(\mathbf{c}; \mathbf{x}) + \lambda \text{Div}(\widehat{\mathcal{C}}) \text{ s.t. } |\widehat{\mathcal{C}}| = K, \text{Valid} = 1 \forall \mathbf{c}. \quad (2)$$

The first term accumulates a success proxy u over selected configurations, where u may be a calibrated yield predictor, a feasibility score, or a learned pairwise preference aggregator. The diversity term Div promotes coverage

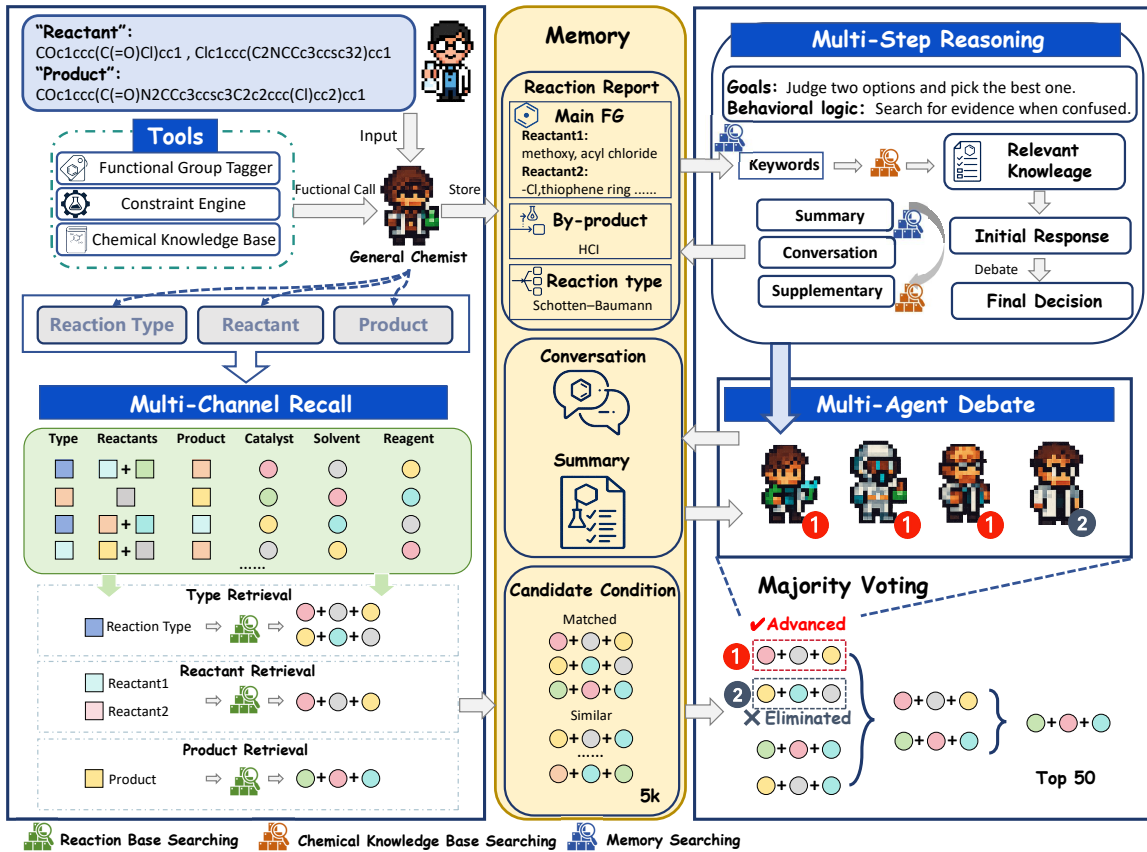


Figure 2: Architecture of ChemMAS. The left side shows how the General Chemist processes SMILES and Multi-Channel Recall retrieves reaction conditions from the Reaction Base. On the right, candidate conditions are paired and evaluated through Multi-Agent Debate, where four agents with Multi-Step Reasoning select the top-50 conditions via Tournament Selection.

across condition dimensions to avoid mode collapse, λ controls the trade-off between utility and diversity. The constraints enforce a fixed budget K and require every selected configuration to be valid, upgrading recommendation to reasoning by demanding justified and verifiable outputs. Classical recommendation optimizes u only. Our task requires each proposed c to carry a falsifiable, evidence-aligned certificate $\rho(c)$.

2.2 OVERVIEW

As illustrated in **Figure 2**, ChemMAS realizes the proposed reasoning framework through a multi-stage agent-based pipeline, with intermediate representations stored in a shared memory. The process begins with a General Chemist that parses the input reaction (\mathcal{R}, \mathcal{P}) using domain-specific tools to extract mechanistic signals, align stoichiometry, and predict reaction type. Outputs are structured into a Reaction Report written to memory. Condition hypotheses are generated via the Multi-Channel Recall module, which independently queries a historical condition database using reaction type, reactant, and product features, followed by combinatorial synthesis into candidate sets of similar conditions. The Tournament Selection phase ranks these candidates through pairwise comparisons conducted by specialized agents, each focusing on one condition dimension (e.g., catalyst, solvent, reagent) under context-aware constraints. Finally, each agent engages in Multi-Step Reasoning over memory and retrieved evidence, and the Multi-Agent Debate aggregates these judgments via majority voting to produce K verified configurations $\{c_1, \dots, c_K\}$, each paired with a rationale $\rho(c)$.

2.3 GENERAL CHEMIST

Given a chemical reaction specified by Reactant SMILES $\mathcal{R} = \{r_i\}$ and Product SMILES $\mathcal{P} = \{p_j\}$, the General Chemist (\mathcal{A}_{Gen}) extracts mechanistically informative priors for downstream condition prediction. The *General Chemist* agent orchestrates three tools, including *Functional Group Tagger*, *Constraint Engine*, and *Chemical Knowledge Base*, to (i) identify main functional groups, (ii) infer balanced stoichiometry and by-products, and (iii) retrieve reaction-type evidence. All outputs are written to *Memory*.

174 **Functional Group Tagger.** A curated library $\mathbb{L} = \{(name_k, \text{SMARTS}_k)\}$ of common organic motifs (e.g.,
 175 acyl chlorides, amines, alcohols, heteroaromatics) is used to match each r_i via SMARTS substructure search,
 176 yielding $\mathcal{F}(r_i)$. The union $\mathcal{F}_{\mathcal{R}} = \bigcup_i \mathcal{F}(r_i)$ is then ranked by role salience considering electrophile/nucleophile
 177 tags, activation levels, and motif frequency across reactants. The top-ranked entries are designated as the Main
 178 FG set and stored in Memory with atom indices for downstream reference.

179 **Constraint Engine.** Reactant and product molecular graphs are canonicalized (including implicit hydrogens),
 180 aligned by maximum common substructure to derive an atom mapping. An integer linear program computes
 181 stoichiometric coefficients $\nu = (\nu_{\mathcal{R}}, \nu_{\mathcal{P}}, \nu_{\text{aux}})$. Changes on mapped atoms, combined with heuristic leaving-
 182 group rules, are used to enumerate neutral species \mathcal{B} , from which the most parsimonious by-product hypothesis is
 183 selected. Both the balanced equation and consistency diagnostics are written to Memory.

184 **Chemical Knowledge Base.** Query templates built from $\mathcal{F}_{\mathcal{R}}$, product scaffolds, and molecular identifiers are
 185 used to retrieve supporting evidence from public repositories (e.g., PubChem) and a locally indexed mirror. Retrieved
 186 exemplars and co-occurrence statistics yield signal features $\mathbf{s}_{\text{ckb}} = \{s_{\text{type}}, s_{\text{role}}, s_{\text{byprod}}\}$, which support
 187 reaction type classification and by-product confirmation. The resulting labels, along with citation metadata, are
 188 stored in Memory for use in later reasoning stages.

191 2.4 MULTI-CHANNEL RECALL

192 We maintain a structured Reaction Base $\mathcal{D} = \{(\tau_n, \mathbf{r}_n, \mathbf{p}_n, \mathbf{c}_n)\}_{n=1}^N$, where each entry contains the reaction type
 193 τ_n , molecular representations of reactants \mathbf{r}_n and products \mathbf{p}_n , and a condition triple $\mathbf{c}_n = (\text{cat}, \text{sol}, \text{reag})$. Given
 194 the current reaction context $(\hat{\tau}, \mathcal{R}, \mathcal{P})$ from Memory, we perform three parallel queries including type-, reactant-,
 195 and product-centric, to obtain candidate index sets $\mathcal{S}_t, \mathcal{S}_r, \mathcal{S}_p$ (exact type match for \mathcal{S}_t , top- k nearest neighbors by
 196 functional-group, MCS, and embedding accuracy for \mathcal{S}_r and \mathcal{S}_p). Without any scoring or rank fusion, an entry is
 197 admitted into *Matched Conditions* if it hits on *any* of the three tags. We define the unified retrieval result as the
 198 deduplicated union:
 199

$$\mathcal{S}_{\text{matched}} = \text{dedup}(\mathcal{S}_t \cup \mathcal{S}_r \cup \mathcal{S}_p), \quad (3)$$

200 and collect $\{\mathbf{c}_n : n \in \mathcal{S}_{\text{matched}}\}$ as experience-driven condition proposals. Optional feasibility filters, e.g.,
 201 mass/charge balance, known by-product constraints, can be applied to screen out invalid entries. To promote
 202 diversity, we construct *Similar Conditions* via applying controlled slot-level recombination $\Pi(\mathbf{c})$ that replaces one
 203 or two elements of \mathbf{c} with high co-occurrence alternatives conditioned on $(\hat{\tau}, \mathcal{F}_{\mathcal{R}})$, while removing infeasible or
 204 near-duplicate combinations. The overall candidate pool is the truncated union:
 205

$$\mathcal{C} = \text{truncate}_{5000}(\mathcal{S}_{\text{matched}} \cup \mathcal{S}_{\text{similar}}), \quad (4)$$

207 which is forwarded to downstream selection and debate.

209 2.5 CANDIDATE PAIRING AND TOURNAMENT SELECTION

210 We refine the initial pool of 5,000 *Candidate Conditions* into a final *Top-50* via a tournament-style knock-
 211 out that emphasizes head-to-head preference (Liu et al., 2025) under comparable context rather than brittle
 212 global scoring. Let $\mathcal{C} = \{\mathbf{c}_i\}_{i=1}^{5000}$. We apply a random permutation π and form disjoint pairs $\mathcal{P}^{(0)} =$
 213 $\{(\mathbf{c}_{\pi(1)}, \mathbf{c}_{\pi(2)}), \dots, (\mathbf{c}_{\pi(4999)}, \mathbf{c}_{\pi(5000)})\}$. In round t , each pair $(\mathbf{a}, \mathbf{b}) \in \mathcal{P}^{(t)}$ is adjudicated by an agent panel,
 214 and the winner is determined by majority vote:
 215

$$\text{win}(\mathbf{a}, \mathbf{b}) = \arg \max_{\mathbf{o} \in \{\mathbf{a}, \mathbf{b}\}} \sum_j \mathbb{1}[d_j = \mathbf{o}], \quad (5)$$

216 with a confidence-sum tie-break when necessary. Winners form $\mathcal{W}^{(t)} = \{\text{win}(\mathbf{a}, \mathbf{b})\}$, which is reshuffled and
 217 re-paired to yield $\mathcal{P}^{(t+1)} = \text{pair}(\text{shuffle}(\mathcal{W}^{(t)}))$. Iteration stops when $|\mathcal{W}^{(T)}| = 50$. We prefer this pairing-and-
 218 knockout protocol to global scoring since absolute scores are difficult to calibrate across heterogeneous condition
 219 sets and amplify noise in near-ties; head-to-head comparison avoids global calibration, anchors judgments in
 220 matched contexts, and affords linear-time selection with natural parallelism.

224 2.6 MULTI-AGENT DEBATE

225 **Multi-Step Reasoning.** For a candidate option $\mathbf{o} \in \{\mathbf{a}, \mathbf{b}\}$, each agent $\mathcal{A}_{\text{Full}}, \mathcal{A}_{\text{Cat}}, \mathcal{A}_{\text{Sol}}, \mathcal{A}_{\text{Rea}}$ executes an
 226 evidence-seeking chain. The agent parses the Memory *Reaction Report* (main functional groups, by-product,
 227 reaction type) to extract keywords κ_j , queries the Chemical Knowledge Base to obtain support $\Theta_j^{(0)}(\mathbf{o})$, and
 228 composes an initial assessment

$$\text{Init}_j(\mathbf{o}) = \text{LLM}(\kappa_j, \Theta_j^{(0)}(\mathbf{o}), \text{structured format}). \quad (6)$$

232 Across micro-rounds $u = 0, \dots, U - 1$, the agent refines its stance by reading peer summaries from the conversation
 233 buffer and re-querying when uncertainty is detected:

$$235 \quad \text{Dec}_j^{(u+1)}(\mathbf{o}) = \Phi\left(\text{Dec}_j^{(u)}(\mathbf{o}), \text{Peers}^{(u)}, \Theta_j^{(u+1)}(\mathbf{o})\right), \quad (7)$$

236 where $\Phi(\cdot)$ integrates new citations, Constraint-Engine checks (e.g., base required to capture HCl), and potential
 237 failure modes. Upon convergence or budget exhaustion, the agent outputs a *final decision* $d_j \in \{\mathbf{a}, \mathbf{b}\}$ with
 238 rationale saved to Memory.

240 **Majority Voting.** After each agent completes Multi-Step Reasoning for both \mathbf{a} and \mathbf{b} , the panel engages in a
 241 structured debate: agents post final assessments and key citations to a shared Memory board, while a designated
 242 facilitator enforces turn-taking and prompts resolution of conflicts (e.g., solvent polarity vs. nucleophile strength).
 243 The pairwise outcome is determined by majority voting as in

$$245 \quad \text{win}(\mathbf{a}, \mathbf{b}) = \arg \max_{\mathbf{o} \in \{\mathbf{a}, \mathbf{b}\}} \sum_j \mathbb{1}[d_j = \mathbf{o}], \quad (8)$$

247 with confidence-sum tie-breaks if needed. The winning option advances to the next tournament round, losers are
 248 eliminated, and iterating over reshuffled winners progressively reduces the 5k candidates to the *Top-50*.

249 3 TWO-STAGE MULTI-TOOL COLLABORATIVE TRAINING FRAMEWORK

251 3.1 CHEMICAL TEACHING

253 We adopt a cold-start Supervised Fine-Tuning (SFT) recipe to endow the backbone LLM with initial Tool-
 254 Integrated Reasoning (TIR) (Dong et al., 2025) for chemical condition judgment. Given training pairs (x_i, y_i) , we
 255 apply the standard Supervised Fine-tuning objective on the backbone model P_θ with parameters θ :

$$257 \quad \mathcal{L}(\theta) = - \sum_{(x_i, y_i)} \log P_\theta(y_i | x_i), \quad (9)$$

259 where x_i denotes the input prompt containing a reaction and paired candidate conditions, and y_i is a structured
 260 target consisting of (i) y_i^r : a step-wise chain that incorporates tool invocation logic and special tokens. (ii)
 261 y_i^a : a concise Judgement section that independently critiques each response and declares the preferred option.
 262 The reasoning trajectory integrates two types of tools, namely *Chemical Knowledge Base searching* and *Memory*
 263 *searching*, serialized in special formats (e.g., `<search>...</search>`, `<memory>...</memory>`), enabling
 264 the model to learn the fundamental rules of tool invocation during the SFT process. Ultimately, this process yields
 265 a cold-start LLM $\hat{\pi}_\theta$ that learns when and how to invoke chemical tools, thereby establishing an initial capability
 266 for TIR in chemistry.

267 3.2 TOOL INCENTIVIZATION

269 After obtaining the cold-start model $\hat{\pi}_\theta$ via SFT, we apply tool incentivization RL to align the policy with both
 270 answer correctness and collaborative tool usage, obtaining π_θ^{RL} .

272 **Hierarchical Reward.** Given a valid format, we augment task accuracy Acc with a multi-tool bonus r_M when
 273 both tools appear (Dong et al., 2025), otherwise we down-weight:

$$275 \quad R = \begin{cases} \max(\text{Acc} + r_M, \text{Acc}), & \text{Format ok and Acc} > 0, \\ 0, & \text{Format ok and Acc} = 0, \\ -1, & \text{Otherwise,} \end{cases} \quad (10)$$

$$279 \quad r_M = \begin{cases} 0.1, & \exists (\text{<search>} \& \text{<memory>}), \\ 0, & \text{otherwise.} \end{cases}$$

282 This explicitly rewards combined tool use without sacrificing correctness.

284 **Tool-Incentivization RL.** For each query q and tool-augmented output o , we adopt Group Relative Policy Opti-
 285 mization (GRPO) (Shao et al., 2024) as our RL algorithm, which *estimates the baseline using a group of rollouts*.
 286 Concretely, we sample G rollouts $\{o_i\}_{i=1}^G$, compute group-normalized advantages with a group baseline, and
 287 optimize

$$288 \quad \mathcal{L}_{\text{GRPO}}(\theta) = \mathbb{E} \left[\frac{1}{G} \sum_{i=1}^G \frac{1}{|o_i|} \sum_{t=1}^{|o_i|} \min(\rho_{i,t} \hat{A}_{i,t}, \text{clip}(\rho_{i,t}, 1 - \epsilon, 1 + \epsilon) \hat{A}_{i,t}) - \beta \text{D}_{\text{KL}}[\hat{\pi}_\theta \parallel \hat{\pi}_{\text{ref}}] \right], \quad (11)$$

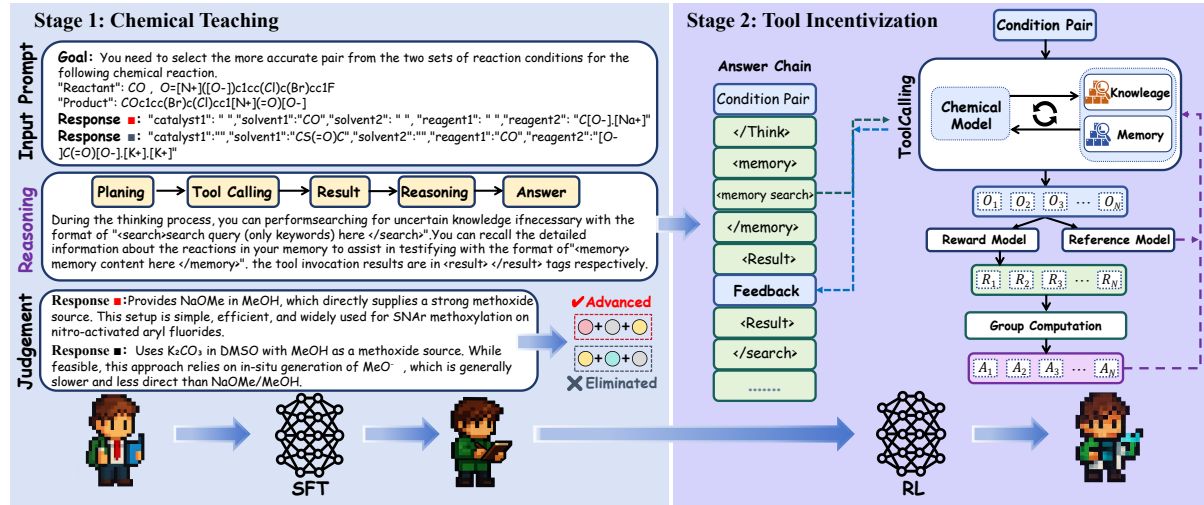


Figure 3: Two-stage Multi-tool Collaborative Training Framework of ChemMAS. Chemical Teaching uses SFT for cold-start training, enabling the LLM to master TIR, and Tool Incentivization employs RL to align the model’s policy with both answer correctness and collaborative tool usage.

where

$$\rho_{i,t}(\theta) = \frac{\hat{\pi}_\theta(o_{i,t} \mid q, o_{i,< t})}{\hat{\pi}_{\text{old}}(o_{i,t} \mid q, o_{i,< t})}, \quad (12)$$

ϵ controls PPO clipping, β weights the KL regularization to the fixed reference $\hat{\pi}_{\text{ref}}$, and $\hat{A}_{i,t}$ denotes the advantage normalized with respect to the group baseline.

4 EXPERIMENTAL SETTINGS

4.1 TRAINING AND EVALUATION SETTING

All agents in ChemMAS are initialized from the same backbone, Qwen3-8B-Instruct, and are trained under a unified *Two-stage Multi-tool Collaborative Training Framework* that applies SFT and RL; while the optimization protocol is shared, the learning objectives and accessible tools differ across agents. We independently trained two distinct models: one for the \mathcal{A}_{Gen} , and another for the multi-agent system comprising $\mathcal{A}_{\text{Full}}$, \mathcal{A}_{Cat} , \mathcal{A}_{Sol} , \mathcal{A}_{Rea} . More training details are in the Appendix.

We measure performance using *Top- k Similarity*, defined as the maximum Tanimoto similarity between the ground truth and top- k predicted candidates, averaged over a composite of molecular fingerprints (Path-based, MACCS, Morgan). This metric reflects the best structural match retrieved by the model. Details are in the Appendix.

4.2 DATASETS

We curate a private dataset of organic reactions, consisting of 544,591 entries represented as reaction equations in SMILES format. For each entry, the *reactants* and *products* are defined as the input, while the reaction conditions, including *catalyst1*, *solvent1*, *solvent2*, *reagent1*, and *reagent2*, are defined as the output. Based on this setting, we construct question–answer pairs and split the dataset into training, validation, and test sets with a ratio of 8:1:1.

Furthermore, we incorporated the RCR subset of ChemCoTBench (Li et al., 2025) as a lightweight public benchmark for small-scale evaluation. This subset of 90 high-quality, well-structured reaction–condition QA instances allows us to assess system generalization and stability under distribution shift. Further details on the private dataset and the ChemCoTBench-RCR subset are provided in the Appendix.

5 RESULTS AND DISCUSSIONS

5.1 MAIN RESULTS

We assessed our proposed method, ChemMAS, against a selection of current models. We compared with specialized chemical models including RCR (Gao et al., 2018), Reagent Transformer (Andronov et al., 2023), and MM RCR (Zhang et al., 2024b), which represent the latest advances in reaction-specific prediction. In addition, we benchmarked against general-purpose large language models (LLMs), such as Qwen3-235B-A22B (Yang et al.,

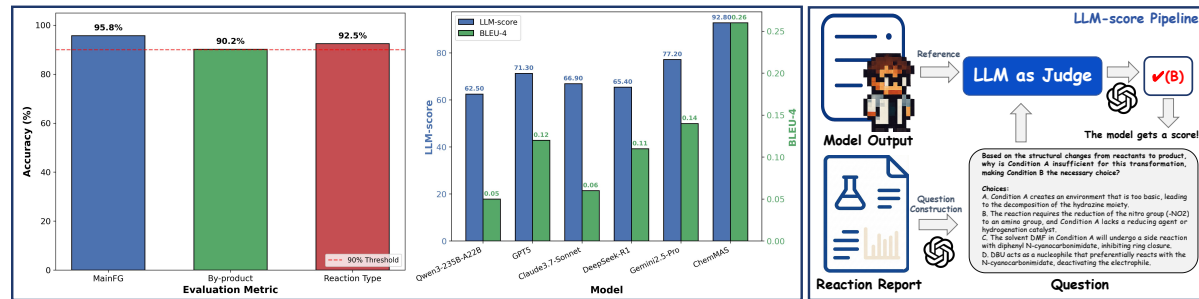


Figure 4: Model Interpretability Evaluation and Scoring Methodology. (Left) Accuracy of ChemMAS outputs compared to human expert annotations. (Center) Human alignment performance comparison; blue bars indicate LLM-Scores and green bars indicate BLEU-4 scores. (Right) Schematic representation of the LLM-Score pipeline and the question-answering based evaluation workflow.

2025), GPT5 (OpenAI), Claude 3.7 Sonnet (Anthropic, 2024), DeepSeek-R1 (Guo et al., 2025), and Gemini2.5-Pro (Comanici et al., 2025), which epitomize the cutting edge in general reasoning and knowledge transfer.

As shown in Table 2, ChemMAS surpasses both specialized chemical models and state-of-the-art LLMs across all reaction types and Top- k settings. It achieves relative Top-1 similarity improvements ranging from 70% to over 90% when compared to domain-specific baselines such as RCR, Reagent Transformer, and MM RCR. Even against top-tier general-purpose LLMs like GPT-5 and Gemini 2.5-Pro, ChemMAS yields consistent relative gains of 15–25% in Top-1 similarity, underscoring its strength in fine-grained mechanistic reasoning.

As shown in Table 2, ChemMAS surpasses both specialized chemical models and state-of-the-art LLMs across all reaction types and Top- k settings. It achieves relative Top-1 similarity improvements ranging from 70% to over 90% when compared to domain-specific baselines such as RCR, Reagent Transformer, and MM RCR. Even against top-tier general-purpose LLMs like GPT-5 and Gemini 2.5-Pro, ChemMAS yields consistent relative gains of 15–25% in Top-1 similarity, underscoring its strength in fine-grained mechanistic reasoning.

Table 1: Generalization evaluation on ChemCoTBench. Top- k similarity (%) for $k \in \{1, 5, 10\}$. The best and second-best results are **bolded** and underlined. Green values in parentheses show relative improvements over the second-best results.

Model	Top- k Similarity (%)									
	Catalyst			Solvent			Reagent			
1	5	10	1	5	10	1	5	10	1	10
Zero-shot LLMs										
Qwen3-235B-A22B	40.1	53.1	58.6	36.4	41.1	52.9	36.4	50.2	58.7	
GPT5	41.9	59.2	66.1	<u>44.1</u>	57.5	65.2	40.1	<u>55.1</u>	61.1	
Claude3.7-Sonnet	38.5	56.2	59.1	40.4	52.1	61.2	34.3	48.0	54.3	
DeepSeek-R1	39.7	55.6	62.0	38.4	48.3	56.3	35.2	47.6	55.4	
Gemini2.5-Pro	<u>45.6</u>	<u>62.1</u>	<u>69.5</u>	42.1	<u>58.6</u>	<u>71.2</u>	38.9	52.1	59.8	
ChemMAS	62.1	68.3	76.1	57.8	66.5	76.8	51.2	59.1	67.7	
	(+16.5)	(+6.2)	(+6.6)	(+13.7)	(+7.9)	(+5.6)	(+11.1)	(+4.0)	(+6.6)	

5.2 GENERALIZATION EVALUATION ON OUT-OF-DISTRIBUTION DATA

To rigorously evaluate the generalization capability of our framework and assess chemical reasoning in out-of-distribution (OOD) scenarios, we conducted additional experiments on ChemCoTBench, a standardized benchmark. The primary objective of this experiment is to verify that ChemMAS does not merely rely on retrieving near-duplicate samples from the knowledge base, but truly possesses the ability to perform robust reasoning on novel reaction types.

Specifically, in the challenging Top-1 setting, as shown in Table 1, ChemMAS achieves a significant accuracy advantage. For catalyst prediction, ChemMAS attains an accuracy of 62.1%, surpassing the second-best model (Gemini 2.5-Pro) by a margin of 16.5%. Similarly, for solvent and reagent prediction, ChemMAS outperforms the strongest competitor (GPT5) by 13.7% and 11.1%, respectively. These substantial performance gains on OOD data demonstrate that our ChemMAS framework effectively generalizes beyond the training distribution, exhibiting fine-grained mechanistic reasoning rather than relying solely on memory-based retrieval.

5.3 EVALUATION OF MODEL INTERPRETABILITY

To ensure the interpretability of ChemMAS, we conducted a two-level evaluation focusing on mechanistic grounding and reasoning quality. First, we validated the intermediate outputs of the General Chemist against human ground truth (Figure 4, Left). The agent demonstrates high reliability, achieving accuracies of 95.8% (MainFG), 90.2% (By-product), and 92.5% (Reaction Type), consistently surpassing the 90% threshold. This high alignment confirms that the system builds its downstream reasoning on a correct and verifiable mechanistic understanding.

406
 407 Table 2: Main results on the private dataset. We report the Top- k similarity (%) across five reaction condition
 408 types: catalyst, solvent1, solvent2, reagent1, and reagent2. Results are evaluated at $k \in \{1, 5, 10\}$. The best and
 409 second-best results are **bolded** and underlined. **Green values** in parentheses indicate relative improvements over
 410 the second-best results.

412 413 414 415 Model	416 417 418 419 420 421 422 423 424 425 426 427 428 429 430 431 432 433 434 435 436 437 438 439 440 441 442 443 444 445 446 447 448 449 450 451 452 453 454 455 456 457 458 459 460 461 462 463 Top- k Similarity (%)														
	Catalyst			Solvent1			Solvent2			Reagent1			Reagent2		
	1	5	10	1	5	10	1	5	10	1	5	10	1	5	10
<i>Pretrained Models</i>															
RCR	40.3	52.6	60.7	49.9	62.1	68.5	45.3	52.8	60.3	50.1	56.2	63.3	36.4	43.3	44.9
Reagent Transformer	35.3	49.3	56.6	38.2	46.3	52.3	37.7	46.4	54.3	46.3	61.3	64.2	37.9	40.1	47.2
MM RCR	43.4	60.1	75.9	53.7	70.7	73.7	49.3	56.3	65.6	55.7	65.2	71.6	40.2	56.3	59.6
<i>Zero-shot LLMs</i>															
Qwen3-235B-A22B	55.4	75.2	77.9	64.0	70.6	73.7	48.4	58.6	64.2	68.3	76.2	82.7	44.2	57.7	60.2
GPT5	62.7	74.2	<u>83.2</u>	<u>73.7</u>	<u>83.7</u>	86.2	65.9	74.3	83.6	67.2	<u>86.9</u>	<u>90.1</u>	68.4	84.9	86.1
Claude3.7-Sonnet	43.6	52.9	60.1	46.0	<u>55.7</u>	58.7	39.2	45.7	53.9	52.3	63.9	67.1	46.2	52.3	54.7
DeepSeek-R1	52.8	69.4	73.2	67.2	73.5	78.1	45.2	54.9	62.2	60.4	71.4	75.7	53.6	67.6	72.3
Gemini2.5-Pro	63.4	<u>79.4</u>	80.5	68.0	83.6	<u>86.4</u>	63.1	74.0	78.6	64.3	82.6	<u>90.1</u>	63.7	76.8	82.2
ChemMAS	78.1	92.3	96.3	85.4	93.9	96.9	76.3	83.2	93.1	88.3	93.6	94.3	73.6	85.2	87.7
	(+14.7)	(+12.9)	(+13.1)	(+11.7)	(+10.2)	(+10.5)	(+10.4)	(+8.9)	(+9.5)	(+20.0)	(+6.7)	(+4.2)	(+5.2)	(+0.3)	(+1.6)

427
 428 Table 3: Ablation on different components in ChemMAS. The best and second-best results are **bolded** and
 429 underlined.

430 431 432 433 434 435 436 437 438 439 440 441 442 443 444 445 446 447 448 449 450 451 452 453 454 455 456 457 458 459 460 461 462 463 Method	431 432 433 434 435 436 437 438 439 440 441 442 443 444 445 446 447 448 449 450 451 452 453 454 455 456 457 458 459 460 461 462 463 Top- k Similarity (%)														
	Catalyst			Solvent 1			Solvent 2			Reagent 1			Reagent 2		
	1	5	10	1	5	10	1	5	10	1	5	10	1	5	10
Memory	w/o Main FG			66.7 82.6 87.6 65.9 76.3 82.7 63.1 70.5 76.8 64.1 76.9 87.6 60.7 65.7 72.3											
	w/o By-Product			70.3 88.4 90.1 78.4 84.1 89.6 69.7 76.0 85.9 74.5 82.8 90.1 68.2 74.9 81.6											
	w/o Reaction Type			<u>74.6</u> 88.6 92.5 <u>82.4</u> 91.6 <u>93.8</u> 73.8 78.6 86.9 81.6 <u>90.3</u> <u>92.0</u> 70.0 78.1 <u>85.3</u>											
Framework	w/o Multi-Agent Debate			65.7 77.9 80.1 66.2 74.1 80.3 58.3 68.2 74.6 62.9 75.6 80.1 52.6 62.0 69.8											
	w/o Multi-Step Reasoning			62.4 79.8 83.5 70.5 79.3 87.5 62.5 72.5 81.3 69.1 84.3 87.2 61.3 72.5 79.8											
	w/o Candidate Pairing			74.1 89.7 92.6 81.6 90.1 92.5 72.8 80.4 89.8 84.2 89.3 91.5 <u>71.4</u> 79.4 82.8											
ChemMAS	78.1	92.3	96.3	85.4	93.9	96.9	76.3	83.2	93.1	88.3	93.6	94.3	73.6	85.2	87.7

444 Building on this foundation, we assessed the quality of the generated reasoning trajectories using a dual-metric
 445 framework comprising BLEU-4 and a semantic **LLM-Score** (Figure 4, Right). The LLM-Score employs an
 446 “LLM-as-a-Judge” mechanism to verify if the generated rationale logically supports expert-derived QA pairs. As
 447 shown in Figure 4 (Center), ChemMAS significantly outperforms general-purpose LLMs, achieving a superior
 448 LLM-Score of 92.8 compared to the 62.5–77.2 range of baselines like DeepSeek-R1 and GPT-5. This substantial
 449 gap, alongside a BLEU-4 score of 0.26, demonstrates that ChemMAS generates scientifically sound explanations
 450 rather than merely plausible text.

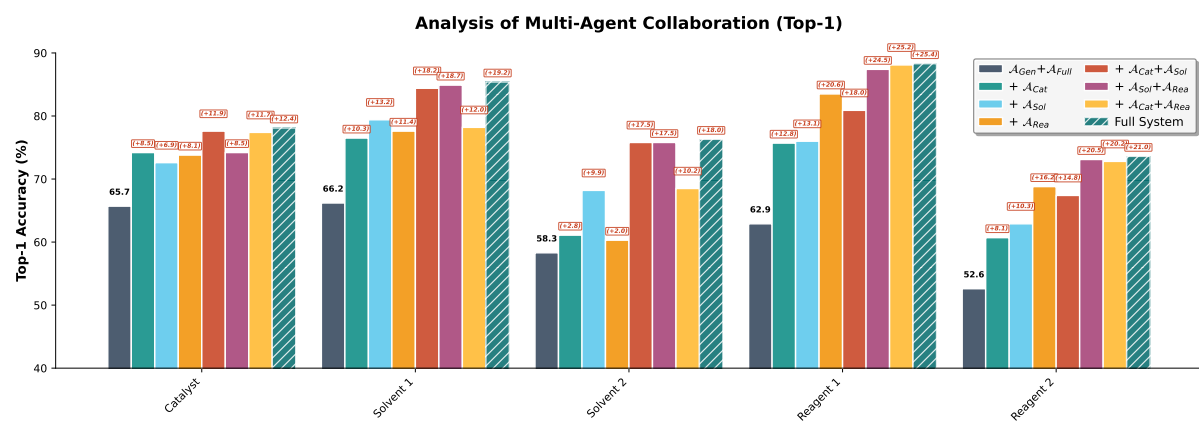
5.4 GENERALIZATION EVALUATION ON OUT-OF-DISTRIBUTION DATA

5.5 ADDITIONAL QUANTITATIVE ANALYSIS

455 **Ablation Studies.** We conducted an ablation study to analyze the contribution of different components in Chem-
 456 MAS. The ablation settings are as follows: (1) w/o Main FG, w/o By-Product, and w/o Reaction Type denote
 457 removing the corresponding elements from the Memory module; (2) w/o Multi-Agent Debate replaces multi-
 458 agent collaboration with a single-agent reasoning process, thereby eliminating conversational exchanges; (3) w/o
 459 Multi-Step Reasoning removes the iterative evidence-based reasoning chain within each agent, such that agents
 460 can only rely on prior knowledge and inter-agent debate without tool invocation; (4) w/o Candidate Pairing dis-
 461 cards the pairwise elimination mechanism for candidate conditions, instead applying a global scoring and ranking
 462 procedure to directly select the top-50 candidates. As illustrated in **Table 3**, removing key components leads to
 463 substantial performance drops, underscoring their critical role in ChemMAS. Specifically, removing Main FG
 464 from the Memory module results in a significant decrease in performance, with an average drop of +8.4% across

464 Table 4: **Ablation study on the SFT, RL, and specific components of the hierarchical reward function, including**
 465 **Acc and r_M . The best and second-best results are **bolded** and underlined.**

Training Framework	Top- k Similarity (%)														
	Catalyst			Solvent 1			Solvent 2			Reagent 1			Reagent 2		
	1	5	10	1	5	10	1	5	10	1	5	10	1	5	10
w/o RL	70.6	88.3	90.4	82.6	89.4	90.5	71.2	80.4	88.5	84.1	87.5	90.2	70.2	82.3	84.5
w/o SFT	67.9	84.3	90.5	81.3	84.6	88.4	72.6	78.1	87.4	79.2	83.5	91.9	67.7	80.9	83.2
w/o Acc	<u>72.6</u>	<u>90.8</u>	<u>93.7</u>	<u>84.1</u>	<u>91.8</u>	<u>92.1</u>	<u>76.0</u>	<u>81.6</u>	<u>91.3</u>	<u>86.7</u>	<u>90.1</u>	<u>92.0</u>	<u>72.5</u>	<u>84.1</u>	<u>86.0</u>
w/o r_M	71.9	89.5	91.2	83.8	91.5	91.0	73.5	81.5	88.7	84.6	88.6	90.8	71.6	82.9	84.9
SFT+RL	78.1	92.3	96.3	85.4	93.9	96.9	76.3	83.2	93.1	88.3	93.6	94.3	73.6	85.2	87.7



492 Figure 5: Multi-agent ablation: Top-1 similarity improvements across Catalyst, Solvent1/2, and Reagent1/2 when
 493 adding specialized agents on top of $\mathcal{A}_{Gen} + \mathcal{A}_{Full}$.

495 all reaction conditions, highlighting the crucial role of functional group extraction and analysis in reaction condition prediction. Similarly, removing Multi-Step Reasoning causes an average similarity decrease of 12.3%, underscoring the importance of evidence-based multi-round reasoning.

499 To evaluate our framework, we ablated SFT, RL, and specific hierarchical reward components. As shown in
 500 Table 4, removing SFT or RL significantly degrades Top- k Similarity across all conditions. Notably, excluding
 501 SFT causes a larger drop than removing RL, underscoring the importance of SFT for initialization. We further
 502 investigated the reward terms in Eq. (10) by removing task accuracy (Acc) and the multi-tool bonus (r_M). Results
 503 show that ablating r_M impairs performance, validating the explicit reward for combined tool usage. Similarly,
 504 excluding Acc degrades results, confirming that prioritizing correctness is essential. These findings validate our
 505 two-stage framework and hierarchical reward design, where all components play complementary roles.

506

507 **Analysis of Multi-Agent Collaboration.** To assess the utility and synergy of different agents, we evaluate combinations built on the base $\mathcal{A}_{Gen} + \mathcal{A}_{Full}$, which are listed in Figure 5. Introducing specialized agents yields improvements. Specifically, \mathcal{A}_{Cat} enhances performance on Catalyst, with an average Top-1 increase of 8.5%. \mathcal{A}_{Sol} shows strong contributions on Solvent1/2, with an average Top-1 gain of 11.6%. \mathcal{A}_{Rea} provides the largest gains on Reagent1/2, with an average Top-1 increase of 18.4%. When all three specialized agents are incorporated, the full system achieves macro-average Top-1 increase of 16–19% across all condition types. These results show that the specialized agents contribute substantial, domain-aligned improvements, and multi-agent debate is conducive to enhancing overall performance. For the analysis of Top-5 and Top-10, see the Appendix.

514 6 CONCLUSION

517 We introduce ChemMAS, a multi-agent system reframing reaction condition recommendation as evidence-based
 518 reasoning grounded in domain knowledge, mechanistic constraints, and interpretable evidence. Unlike prediction-
 519 only baselines, ChemMAS explains *why* conditions are appropriate, enhancing trust and utility. Empirically, it
 520 achieves up to 30% Top-1 similarity gains over specialized models and outperforms general LLMs. These results
 521 validate the transition from black-box predictions to auditable decision-making. Future work will extend this
 framework to broader domains such as materials design and bioinformatics.

522 REFERENCES

523 Rizvi Syed Aal E Ali, Jiaolong Meng, Muhammad Ehtisham Ibraheem Khan, and Xuefeng Jiang. Machine
524 learning advancements in organic synthesis: A focused exploration of artificial intelligence applications in
525 chemistry. *Artificial Intelligence Chemistry*, 2(1):100049, 2024.

526

527 Mikhail Andronov, Varvara Voinarovska, Natalia Andronova, Michael Wand, Djork-Arné Clevert, and Jürgen
528 Schmidhuber. Reagent prediction with a molecular transformer improves reaction data quality. *Chemical
529 Science*, 14(12):3235–3246, 2023.

530

531 Anthropic. Claude 3.7 sonnet, 2024. URL [https://www.anthropic.com/news/
532 claude-3-7-sonnet](https://www.anthropic.com/news/claude-3-7-sonnet).

533 Matt Ball, Dragos Horvath, Thierry Kogej, Mikhail Kabeshov, and Alexandre Varnek. Predicting reaction conditions: a data-driven perspective. *Chemical Science*, 2025.

534

535 Daniil A Boiko, Robert MacKnight, Ben Kline, and Gabe Gomes. Autonomous chemical research with large
536 language models. *Nature*, 624(7992):570–578, 2023.

537

538 Andres M Bran, Theo A Neukomm, Daniel P Armstrong, Zlatko Jončev, and Philippe Schwaller. Chemical
539 reasoning in llms unlocks steerable synthesis planning and reaction mechanism elucidation. *arXiv preprint
540 arXiv:2503.08537*, 2025.

541

542 Kexin Chen, Junyou Li, Kunyi Wang, Yuyang Du, Jiahui Yu, Jiamin Lu, Lanqing Li, Jiezhong Qiu, Jianzhang Pan,
543 Yi Huang, et al. Chemist-x: Large language model-empowered agent for reaction condition recommendation
544 in chemical synthesis. *arXiv preprint arXiv:2311.10776*, 2023.

545

546 Gheorghe Comanici, Eric Bieber, Mike Schaeckermann, Ice Pasupat, Noveen Sachdeva, Inderjit Dhillon, Marcel
547 Blstein, Ori Ram, Dan Zhang, Evan Rosen, et al. Gemini 2.5: Pushing the frontier with advanced reasoning,
548 multimodality, long context, and next generation agentic capabilities. *arXiv preprint arXiv:2507.06261*, 2025.

549

550 Guanting Dong, Yifei Chen, Xiaoxi Li, Jiajie Jin, Hongjin Qian, Yutao Zhu, Hangyu Mao, Guorui Zhou, Zhicheng
551 Dou, and Ji-Rong Wen. Tool-star: Empowering llm-brained multi-tool reasoner via reinforcement learning.
552 *arXiv preprint arXiv:2505.16410*, 2025.

553

554 Yilun Du, Shuang Li, Antonio Torralba, Joshua B Tenenbaum, and Igor Mordatch. Improving factuality and
555 reasoning in language models through multiagent debate. In *International Conference on Machine Learning*,
556 2023.

557

558 Carl Edwards, Tuan Lai, Kevin Ros, Garrett Honke, Kyunghyun Cho, and Heng Ji. Translation between molecules
559 and natural language. In *Conference on Empirical Methods in Natural Language Processing*, December 2022.

560

561 Hanyu Gao, Thomas J Struble, Connor W Coley, Yuran Wang, William H Green, and Klavs F Jensen. Using
562 machine learning to predict suitable conditions for organic reactions. *ACS Central Science*, 4(11):1465–1476,
563 2018.

564

565 Luyu Gao, Aman Madaan, Shuyan Zhou, Uri Alon, Pengfei Liu, Yiming Yang, Jamie Callan, and Graham Neubig.
566 Pal: Program-aided language models. In *International Conference on Machine Learning*, pp. 10764–10799,
567 2023.

568

569 Daya Guo, Dejian Yang, Haowei Zhang, Junxiao Song, Ruoyu Zhang, Runxin Xu, Qihao Zhu, Shirong Ma, Peiyi
570 Wang, Xiao Bi, et al. Deepseek-r1: Incentivizing reasoning capability in llms via reinforcement learning. *arXiv
571 preprint arXiv:2501.12948*, 2025.

572

573 Idil Ismail, Raphael Chantreau Majerus, and Scott Habershon. Graph-driven reaction discovery: progress, chal-
574 lenges, and future opportunities. *The Journal of Physical Chemistry A*, 126(40):7051–7069, 2022.

575

576 Dongzhi Jiang, Renrui Zhang, Ziyu Guo, Yanwei Li, Yu Qi, Xinyan Chen, Liuhui Wang, Jianhan Jin, Claire Guo,
577 Shen Yan, et al. Mme-cot: Benchmarking chain-of-thought in large multimodal models for reasoning quality,
578 robustness, and efficiency. *arXiv preprint arXiv:2502.09621*, 2025.

579

580 Lars Benedikt Kaesberg, Jonas Becker, Jan Philip Wahle, Terry Ruas, and Bela Gipp. Voting or consensus?
581 decision-making in multi-agent debate. *arXiv preprint arXiv:2502.19130*, 2025.

582

583 Joshua Ong Jun Leang, Aryo Pradipta Gema, and Shay B Cohen. Comat: Chain of mathematically annotated
584 thought improves mathematical reasoning. *arXiv preprint arXiv:2410.10336*, 2024.

585

586 Minhyeok Lee, Umit V Ucak, Jinyoung Jeong, Islambek Ashyrmamatov, Juyong Lee, and Eunji Sim. Automated
587 and efficient sampling of chemical reaction space. *Advanced Science*, 12(9):2409009, 2025.

580 Hao Li, He Cao, Bin Feng, Yanjun Shao, Xiangru Tang, Zhiyuan Yan, Li Yuan, Yonghong Tian, and Yu Li.
 581 Beyond chemical qa: Evaluating llm's chemical reasoning with modular chemical operations. *arXiv preprint*
 582 *arXiv:2505.21318*, 2025.

583 Tiantao Liu, Zheng Cao, Yuansheng Huang, Yue Wan, Jian Wu, Chang-Yu Hsieh, Tingjun Hou, and Yu Kang.
 584 Syncluster: reaction type clustering and recommendation framework for synthesis planning. *JACS Au*, 3(12):
 585 3446–3461, 2023.

587 Yantao Liu, Zijun Yao, Rui Min, Yixin Cao, Lei Hou, and Juanzi Li. Pairjudge rm: Perform best-of-n sampling
 588 with knockout tournament. *arXiv preprint arXiv:2501.13007*, 2025.

589 George Lyall-Brookes, Alex C Padgham, and Anna G Slater. Flow chemistry as a tool for high throughput
 590 experimentation. *Digital Discovery*, 2025.

592 Andres M. Bran, Sam Cox, Oliver Schilter, Carlo Baldassari, Andrew D White, and Philippe Schwaller. Aug-
 593 menting large language models with chemistry tools. *Nature Machine Intelligence*, 6(5):525–535, 2024.

594 Michael R Maser, Alexander Y Cui, Serim Ryou, Travis J DeLano, Yisong Yue, and Sarah E Reisman. Multilabel
 595 classification models for the prediction of cross-coupling reaction conditions. *Journal of Chemical Information*
 596 and *Modeling*, 61(1):156–166, 2021.

598 Humza Naveed, Asad Ullah Khan, Shi Qiu, Muhammad Saqib, Saeed Anwar, Muhammad Usman, Naveed Akhtar,
 599 Nick Barnes, and Ajmal Mian. A comprehensive overview of large language models. *ACM Transactions on*
 600 *Intelligent Systems and Technology*, 16(5):1–72, 2025.

602 OpenAI. Gpt-5 system card. URL <https://openai.com/index/gpt-5-system-card/>.

603 Yujie Qian, Zhening Li, Zhengkai Tu, Connor Coley, and Regina Barzilay. Predictive chemistry augmented with
 604 text retrieval. In Houda Bouamor, Juan Pino, and Kalika Bali (eds.), *Conference on Empirical Methods in*
 605 *Natural Language Processing*, pp. 12731–12745, December 2023.

607 Zhihong Shao, Peiyi Wang, Qihao Zhu, Runxin Xu, Junxiao Song, Xiao Bi, Haowei Zhang, Mingchuan Zhang,
 608 YK Li, Yang Wu, et al. Deepseekmath: Pushing the limits of mathematical reasoning in open language models.
 609 *arXiv preprint arXiv:2402.03300*, 2024.

610 Xiangru Tang, Tianyu Hu, Muyang Ye, Yanjun Shao, Xunjian Yin, Siru Ouyang, Wangchunshu Zhou, Pan Lu,
 611 Zhuosheng Zhang, Yilun Zhao, et al. Chemagent: Self-updating library in large language models improves
 612 chemical reasoning. *arXiv preprint arXiv:2501.06590*, 2025.

614 Connor J Taylor, Alexander Pomberger, Kobi C Felton, Rachel Grainger, Magda Barecka, Thomas W Chamber-
 615 iain, Richard A Bourne, Christopher N Johnson, and Alexei A Lapkin. A brief introduction to chemical reaction
 616 optimization. *Chemical Reviews*, 123(6):3089–3126, 2023.

617 Zhengkai Tu, Thijs Stuyver, and Connor W Coley. Predictive chemistry: machine learning for reaction deploy-
 618 ment, reaction development, and reaction discovery. *Chemical science*, 14(2):226–244, 2023.

620 Ashish Vaswani, Noam Shazeer, Niki Parmar, Jakob Uszkoreit, Llion Jones, Aidan N Gomez, Łukasz Kaiser, and
 621 Illia Polosukhin. Attention is all you need. *Advances in neural information processing systems*, 30, 2017.

623 Xiaorui Wang, Chang-Yu Hsieh, Xiaodan Yin, Jike Wang, Yuquan Li, Yafeng Deng, Dejun Jiang, Zhenxing Wu,
 624 Hongyan Du, Hongming Chen, et al. Generic interpretable reaction condition predictions with open reaction
 625 condition datasets and unsupervised learning of reaction center. *Research*, 6:0231, 2023.

626 Junde Wu, Jiayuan Zhu, Yuyuan Liu, Min Xu, and Yueming Jin. Agentic reasoning: A streamlined framework for
 627 enhancing llm reasoning with agentic tools. In *Annual Meeting of the Association for Computational Linguis-
 628 tics*, pp. 28489–28503, 2025.

630 Zonghan Wu, Shirui Pan, Fengwen Chen, Guodong Long, Chengqi Zhang, and Philip S Yu. A comprehensive
 631 survey on graph neural networks. *IEEE transactions on neural networks and learning systems*, 32(1):4–24,
 632 2020.

633 An Yang, Anfeng Li, Baosong Yang, Beichen Zhang, Binyuan Hui, Bo Zheng, Bowen Yu, Chang Gao, Chengen
 634 Huang, Chenxu Lv, et al. Qwen3 technical report. *arXiv preprint arXiv:2505.09388*, 2025.

636 Guibin Zhang, Yanwei Yue, Zhixun Li, Sukwon Yun, Guancheng Wan, Kun Wang, Dawei Cheng, Jeffrey Xu Yu,
 637 and Tianlong Chen. Cut the crap: An economical communication pipeline for llm-based multi-agent systems.
 638 *arXiv preprint arXiv:2410.02506*, 2024a.

638 Yu Zhang, Ruijie Yu, Kaipeng Zeng, Ding Li, Feng Zhu, Xiaokang Yang, Yaohui Jin, and Yanyan
639 Xu. Text-augmented multimodal llms for chemical reaction condition recommendation. *arXiv preprint*
640 *arXiv:2407.15141*, 2024b.

641 Wayne Xin Zhao, Kun Zhou, Junyi Li, Tianyi Tang, Xiaolei Wang, Yupeng Hou, Yingqian Min, Beichen Zhang,
642 Junjie Zhang, Zican Dong, et al. A survey of large language models. *arXiv preprint arXiv:2303.18223*, 1(2),
643 2023.

644 Tianhang Zhou, Yingchun Niu, Xingying Lan, and Chunming Xu. Locally-deployed chain-of-thought (cot) rea-
645 soning model in chemical engineering: Starting from 30 experimental data. *arXiv preprint arXiv:2502.12383*,
646 2025.

647 Kunlun Zhu, Hongyi Du, Zhaochen Hong, Xiaocheng Yang, Shuyi Guo, Zhe Wang, Zhenhailong Wang, Cheng
648 Qian, Xiangru Tang, Heng Ji, et al. Multiagentbench: Evaluating the collaboration and competition of llm
649 agents. *arXiv preprint arXiv:2503.01935*, 2025.

650

651

652

653

654

655

656

657

658

659

660

661

662

663

664

665

666

667

668

669

670

671

672

673

674

675

676

677

678

679

680

681

682

683

684

685

686

687

688

689

690

691

692

693

694

695

696 Supplemental Material of ChemMAS

698 This document provides supplementary material to complement the main paper. It includes detailed descriptions
 699 of the ChemMAS system, prompt templates, training pipeline, additional experimental results, and reproducibility
 700 assets. Specifically:

- 702 • **Appendix A** describes how large language models (e.g., GPT-5 and Google Nano Banana) were used in
 703 writing assistance and figure generation.
- 704 • **Appendix B** provides the reproducibility statement and access link to the code and data repository.
- 705 • **Appendix C** summarizes related works in three areas:
 - 707 – Appendix C.1: Reaction Condition Prediction
 - 708 – Appendix C.2: LLM-Based Multi-Agent Systems
 - 709 – Appendix C.3: LLM-Based Reasoning Models
- 710 • **Appendix D** details the ChemMAS methodology, including:
 - 711 – Appendix D.1: Algorithm of ChemMAS Framework and Multi-Agent Debate
 - 712 – Appendix D.1: Two-Stage Multi-Tool Collaborative Training
- 714 • **Appendix E** outlines the experimental settings, including:
 - 715 – Appendix E.1: Training Pipeline for Agents
 - 716 – Appendix E.2: Evaluation Setting Details (Candidate Ranking)
- 718 • **Appendix F** details the evaluation protocol and metrics:
 - 719 – Appendix F.1: SMILES Canonicalization and Validity
 - 720 – Appendix F.2: Tanimoto Similarity
 - 721 – Appendix F.3: Molecular Fingerprint Types
 - 722 – Appendix F.4: Aggregate Evaluation Metrics and Top-k Similarity
- 724 • **Appendix G** introduces the dataset details:
 - 725 – Appendix G: Public Dataset (ChemCoTBench RCR subset)
 - 726 – Appendix G: Private Dataset curation and statistics
- 728 • **Appendix H** presents the prompt templates for different agents.
- 729 • **Appendix I** presents additional experimental results and discussions:
 - 730 – Appendix I.1: Additional Quantitative Results (Top-5 and Top-10 Analysis)
 - 731 – Appendix I.2: Result Visualization and qualitative analysis

733 A THE USE OF LARGE LANGUAGE MODELS

735 In this work, the large language model GPT-5 was used as a general-purpose tool for polishing the writing, in-
 736 cluding improving clarity and grammar. In Figure 2, the five images representing the agents and small tool icons
 737 were generated with the assistance of GPT-5¹, while the overall framework was created by the authors. The three
 738 images representing different models in Figure 3 were produced with the help of Google Nano Banana². The
 739 conceptual design of both figures were entirely implemented by the authors.

741 B REPRODUCIBILITY STATEMENT

743 We provide complete code, part of data with instructions, which are available at Code

745 C RELATED WORKS

748 C.1 REACTION CONDITION PREDICTION

749 Predicting reaction conditions from reactants and products is a long-standing challenge in computer-aided syn-
 750 thesis. Early large-scale efforts such as (Gao et al., 2018) used feedforward neural networks trained on millions
 751 of Reaxys records to jointly predict catalysts, solvents, reagents, and temperatures, achieving promising top-k

753 ¹<https://chatgpt.com/>

²<https://www.nano-banana.ai/>

754 accuracies despite sparsity and label imbalance. Focusing on cross-coupling families, (Maser et al., 2021) formulated the task as multi-label ranking, developing role-specific encoders and leveraging graph-based features to yield accurate, context-aware predictions. To improve generalization and interpretability, (Wang et al., 2023) released benchmark datasets and proposed Parrot, a Transformer model augmented with unsupervised reaction center learning. Parrot achieved significant gains in condition similarity and temperature estimation while offering interpretable attention maps localized to reactive substructures. Separately, (Andronov et al., 2023) addressed data quality limitations by training a Molecular Transformer to impute missing reagents in USPTO reactions. Their system not only improved reagent recall but also enhanced downstream product prediction models.

762 Retrieval-augmented methods incorporate external knowledge to improve robustness. TextReact (Qian et al., 763 2023) pairs structure-based encoders with retrieved literature snippets to inform condition prediction and retrosynthesis. By integrating textual context into training, it significantly outperforms molecule-only baselines. In 764 peptide catalysis design, (Edwards et al., 2022) proposed a semi-automated ML framework for selecting universal 765 catalyst libraries and discovered novel, high-selectivity peptides via efficient search in a large tripeptide space. At 766 the interface of language and chemistry, (Edwards et al., 2022) introduced MolT5, a pre-trained encoder-decoder 767 model that translates between molecules and natural language. It supports molecule-to-caption generation and 768 chemically constrained text-to-molecule synthesis, offering a foundation for LLM-based explainability. More 769 recently, (Zhang et al., 2024b) proposed a text-augmented multimodal LLM framework for reaction condition 770 recommendation. Their method jointly encodes SMILES, molecular graphs, and relevant text to achieve state-of- 771 the-art similarity across open benchmarks and improve generalization under low-data or OOD settings. Despite 772 these advances, current methods primarily focus on recommending what the potential reaction conditions are, but 773 fail to provide explanatory why-level evidence for why such conditions are important or mechanistically justified.

775 C.2 LLM-BASED MULTI-AGENT SYSTEMS

776 LLMs are increasingly deployed as autonomous agents equipped with retrieval, reasoning, and tool-use capabilities. (Boiko et al., 2023) showcased early efforts in autonomous laboratory control, with LLM agents performing 777 iterative web search, experimental planning, and execution. (M. Bran et al., 2024) extended this direction in chemistry by coupling GPT-4 with 18 specialized tools for retrosynthesis, property prediction, and literature search. The 778 resulting system could autonomously complete multi-step syntheses and identify new chromophores. In reaction 779 condition recommendation, (Chen et al., 2023) leveraged retrieval-augmented generation by combining molecular 780 similarity search, literature parsing, and in silico condition evaluation, mimicking the workflow of expert chemists.

781 To address hallucinations and unreliable reasoning, multi-agent collaboration has emerged as a promising direction. (Du et al., 2023) proposed a multi-agent debate framework where LLMs iteratively critique each other's 782 answers, leading to improved factuality and robustness. (Zhu et al., 2025) benchmarked agent interactions across 783 collaborative and competitive settings, revealing that structured debate and agent role specialization improve task 784 success. Recent work further explores coordination protocols. (Kaesberg et al., 2025) found that consensus-based 785 decision-making outperforms majority voting on complex QA tasks, while (Zhang et al., 2024a) introduced a 786 compression pipeline that reduces inter-agent communication by up to 70% without degrading performance. (Wu 787 et al., 2025) introduced Agentic Reasoning, a general framework for LLMs to call sub-agents (*e.g.*, web search, 788 code execution, memory management), enabling long-horizon, tool-rich scientific workflows. Together, these 789 systems demonstrate that combining LLMs with external tools, structured memory, and agent-level reasoning 790 can produce scalable, verifiable pipelines for high-stakes domains. However, how to enhance the factuality and 791 reliability of reaction condition prediction remains largely unexplored.

800 C.3 LLM-BASED REASONING MODELS

801 A complementary line of work focuses on improving the reasoning capabilities of LLMs, which is essential 802 for high-stakes decision-making and interpretability in scientific domains. In general contexts, program-aided 803 language models (PAL) (Gao et al., 2023) execute intermediate logic through code to improve arithmetic and 804 symbolic reasoning. CoT prompting, self-consistency, and debate-style prompting have shown broad benefits 805 in multi-step question answering. CoMAT (Leang et al., 2024) proposes a mathematically annotated chain-of- 806 thought mechanism to handle complex symbolic queries. MME-CoT (Jiang et al., 2025) benchmarks the reasoning 807 abilities of large multimodal models across science, math, and logic domains. In chemistry, (Tang et al., 2025) 808 introduces a self-updating subtask library to facilitate memory-augmented chemical reasoning. It decomposes 809 complex tasks into reusable subtasks and retrieves relevant solutions, enabling LLMs to generalize over time via 810 experience. However, the ability to infer mechanistic or contextual rationales behind chemical reaction conditions 811 is rarely addressed in existing works.

812 **D METHOD DETAILS**813 **D.1 ALGORITHM OF CHEMMAS FRAMEWORK**

814
Multi-Agent Debate. In this section, we outline the overall workflow of our Multi-Agent Debate procedure.
 815 The process consists of two coordinated phases executed for each candidate pair, as illustrated in **Algorithm 1**
 816 (see also the prompt specification in **Figure 8**):

817 **(1) Evidence-Seeking & Refinement.** Given a pair (a, b) , each agent A_j initializes an evidence-seeking chain by
 818 parsing the *Reaction Report* (main functional groups, by-products, reaction type) to extract keywords, querying
 819 the Chemical Knowledge Base for citations, and composing an initial assessment. Across U micro-rounds, agents
 820 iteratively refine their stance by (i) reading peer summaries from the shared buffer, (ii) re-querying the KB when
 821 uncertainty is detected, and (iii) invoking the Constraint Engine (e.g., verifying that bases are present to capture
 822 HCl). This yields a final per-agent decision $d_j \in \{a, b\}$ with confidence and citations.

823 **(2) Panel Aggregation & Tournament.** After convergence, all agents post their final assessments to the Memory
 824 board. The pairwise winner is determined by *majority voting*; ties are broken by the sum of confidences. Winners
 825 advance while losers are eliminated, and repeated rounds over reshuffled winners progressively reduce the pool to
 826 the *Top-50*. This debate-driven pipeline promotes cross-agent verification, encourages tool-grounded reasoning,
 827 and produces interpretable, citation-backed outcomes archived in Memory.

828 **Two-Stage Multi-Tool Collaborative Training.** In this section, we outline the overall workflow of our Two-
 829 Stage Multi-Tool Collaborative Training pipeline. The procedure alternates two phases over multiple cycles, as
 830 illustrated in **Algorithm 2** (see also the prompt specifications in **Figure 7** and **Figure 8**):

831 **(1) Chemical Teaching (SFT).** Starting from the Qwen3-8B-Instruct backbone, we perform supervised fine-
 832 tuning on structured trajectories that serialize tool invocations (e.g., *search*, *memory*) before the final label. This
 833 phase teaches the model *when* and *how* to call tools and enforces a standardized output format, yielding a cold-
 834 start, tool-aware policy $\hat{\pi}_\theta$.

835 **(2) Tool Incentivization (RL).** Initialized from $\hat{\pi}_\theta$, we optimize the policy with GRPO using a hierarchical reward
 836 that jointly encourages (i) format validity, (ii) answer correctness, and (iii) collaborative multi-tool usage. For
 837 each query, the model samples G tool-augmented rollouts; advantages are normalized with a group baseline and
 838 regularized by a KL term to a frozen reference. Policy parameters are then updated to maximize the GRPO
 839 objective.

840 This alternating scheme combines supervised teaching of tool protocols with reinforcement alignment for similarity
 841 and collaboration, resulting in a robust tool-aware reasoning model π_θ^{RL} with interpretable, consistent behavior.

842 **E EXPERIMENTAL SETTINGS**843 **E.1 TRAINING PIPELINE**

844 For both \mathcal{A}_{Gen} and the multi-agent system, we employ a two-stage optimization strategy consistent with the main
 845 framework. In the SFT stage, the AdamW optimizer is used with $\beta = (0.9, 0.95)$, an initial learning rate of
 846 2×10^{-5} , and a weight decay of 0.1. Each model is trained for one epoch with a batch size of 128. In the
 847 subsequent RL stage, we adopt the GRPO strategy with learning rate 1×10^{-6} , KL coefficient 0.04, and number
 848 of iterations set to 1. To enhance diversity, we set the temperature parameter to 0.75 during generation. All training
 849 and inference are conducted on 8 NVIDIA A100 GPUs.

850 **General Chemist (\mathcal{A}_{Gen}).** The input is limited to *Reactant* and *Product* SMILES, and the output is the predicted
 851 *Reaction Type*. During SFT, the supervision target is structured as a step-wise chain that explicitly serializes
 852 three tool invocations—*Functional Group Tagger*, *Constraint Engine*, and *Chemical Knowledge Base Searching*—
 853 before emitting the final reaction type. This design enables the model to learn *when* and *how* to call tools. In the
 854 subsequent RL stage, we apply a hierarchical reward that integrates format correctness, answer similarity, and
 855 collaborative multi-tool usage.

856 **Multi-Agent System ($\mathcal{A}_{\text{Full}}$, \mathcal{A}_{Cat} , \mathcal{A}_{Sol} , \mathcal{A}_{Rea}).** These role-specialized agents share the same trained back-
 857 bone and are SFT on QA pairs generated in the *Candidate Pairing* stage. The supervision targets embed the
 858 invocation logic of two tools—*Chemical Knowledge Base Searching* and *Memory Searching*. The RL stage em-
 859 ploys the same reward design to align both judgment quality and tool collaboration, ensuring that agents can
 860 deliberate effectively while remaining tool-aware.

Algorithm 1 Multi-Agent Debate with Multi-Step Reasoning and Majority Voting

870 **Require:** Agent set $\mathcal{A} = \{A_1, \dots, A_m\}$; Candidates \mathcal{C} ;
871 Memory: Reaction Report (main_fg, by_product, reaction_type);
872 Chemical Knowledge Base (KB); Constraint Engine; Micro-rounds U ; target $K=50$.
873 **Output:** Top- K surviving candidates

```

874 1: function MAD_TOURNAMENT( $\mathcal{C}, \mathcal{A}, U, K$ )
875 2:   while  $|\mathcal{C}| > K$  do ▷ pairwise tournament until Top- $K$ 
876 3:      $\mathcal{P} \leftarrow \text{PAIRSHUFFLE}(\mathcal{C})$  ▷ form disjoint pairs
877 4:      $\mathcal{C}_{\text{next}} \leftarrow \emptyset$ 
878 5:     for all  $(\mathbf{a}, \mathbf{b}) \in \mathcal{P}$  do
879 6:        $\mathcal{D} \leftarrow \text{DEBATEMATCH}(\mathbf{a}, \mathbf{b}, \mathcal{A}, U)$ 
880 7:        $\mathbf{o}^* \leftarrow \text{MAJORITYVOTE}(\mathcal{D})$  ▷ winner  $\mathbf{a}$  or  $\mathbf{b}$ 
881 8:        $\mathcal{C}_{\text{next}} \leftarrow \mathcal{C}_{\text{next}} \cup \{\mathbf{o}^*\}$ 
882 9:     end for
883 10:     $\mathcal{C} \leftarrow \mathcal{C}_{\text{next}}$ 
884 11:  end while
885 12:  return  $\mathcal{C}$ 
886 13: end function
887 14: function DEBATEMATCH( $\mathbf{a}, \mathbf{b}, \mathcal{A}, U$ )
888 15:    $\mathcal{D} \leftarrow \emptyset$  ▷ per-agent final outputs and confidences
889 16:   for all  $A_j \in \mathcal{A}$  do ▷ each agent reasons on both options
890 17:     for all  $\mathbf{o} \in \{\mathbf{a}, \mathbf{b}\}$  do
891 18:        $\kappa_j \leftarrow \text{EXTRACTKEYWORDS}(\text{Reaction Report})$ 
892 19:        $\Theta_j^{(0)}(\mathbf{o}) \leftarrow \text{QUERYKB}(\kappa_j, \mathbf{o})$ 
893 20:        $\text{Dec}_j^{(0)}(\mathbf{o}) \leftarrow \text{COMPOSEINIT}(\kappa_j, \Theta_j^{(0)}(\mathbf{o}))$ 
894 21:     for  $u = 0$  to  $U-1$  do ▷ micro-round refinement
895 22:        $\text{Peers}^{(u)} \leftarrow \text{READPEERSUMMARIES}(\mathcal{A} \setminus \{A_j\})$ 
896 23:       if DETECTUNCERTAINTY( $\text{Dec}_j^{(u)}(\mathbf{o})$ ,  $\text{Peers}^{(u)}$ ) then
897 24:          $\Theta_j^{(u+1)}(\mathbf{o}) \leftarrow \text{QUERYKB}(\kappa_j, \mathbf{o})$ 
898 25:       else
899 26:          $\Theta_j^{(u+1)}(\mathbf{o}) \leftarrow \Theta_j^{(u)}(\mathbf{o})$ 
900 27:       end if
901 28:        $\Gamma_j^{(u+1)}(\mathbf{o}) \leftarrow \text{CONSTRAINTCHECK}(\mathbf{o}, \text{by\_product=HCl, base-needed, ...})$ 
902 29:        $\text{Dec}_j^{(u+1)}(\mathbf{o}) \leftarrow \text{UPDATEDECISION}(\text{Dec}_j^{(u)}(\mathbf{o}), \text{Peers}^{(u)}, \Theta_j^{(u+1)}(\mathbf{o}), \Gamma_j^{(u+1)}(\mathbf{o}))$ 
903 30:     end for
904 31:   end for
905 32:    $(d_j, c_j, \text{cit}_j) \leftarrow \text{FINALIZE}(\text{Dec}_j^{(U)}(\mathbf{a}), \text{Dec}_j^{(U)}(\mathbf{b}))$ 
906 33:    $\text{Writetomemoryboard}(A_j, d_j, c_j, \text{cit}_j)$  ▷ store rationale/citations
907 34:    $\mathcal{D} \leftarrow \mathcal{D} \cup \{(A_j, d_j, c_j)\}$ 
908 35: end for
909 36: return  $\mathcal{D}$ 
910 37: end function
911 38: function MAJORITYVOTE( $\mathcal{D}$ )
912 39:    $n_{\mathbf{a}} \leftarrow \sum_{(A_j, d_j, c_j) \in \mathcal{D}} \mathbb{1}[d_j = \mathbf{a}]$ ;  $n_{\mathbf{b}} \leftarrow \sum_{(A_j, d_j, c_j) \in \mathcal{D}} \mathbb{1}[d_j = \mathbf{b}]$ 
913 40:   if  $n_{\mathbf{a}} \neq n_{\mathbf{b}}$  then
914 41:     return  $\arg \max_{\mathbf{o} \in \{\mathbf{a}, \mathbf{b}\}} \{n_{\mathbf{o}}\}$ 
915 42:   else ▷ tie-break by confidence sum
916 43:      $s_{\mathbf{a}} \leftarrow \sum_{(A_j, d_j, c_j) \in \mathcal{D}} c_j \cdot \mathbb{1}[d_j = \mathbf{a}]$ 
917 44:      $s_{\mathbf{b}} \leftarrow \sum_{(A_j, d_j, c_j) \in \mathcal{D}} c_j \cdot \mathbb{1}[d_j = \mathbf{b}]$ 
918 45:     return  $\arg \max_{\mathbf{o} \in \{\mathbf{a}, \mathbf{b}\}} \{s_{\mathbf{o}}\}$ 
919 46:   end if
920 47: end function

```

E.2 EVALUATION SETTING DETAILS

921 We evaluate general-purpose LLMs in a controlled candidate-ranking regime aligned with the ChemMAS pipeline.
922 Directly prompting models with only Reactant and Product SMILES yields an excessively large decision space,
923 leading to chemically plausible yet inaccurate suggestions and a Top-1 similarity of approximately 5%. To obtain a
924 faithful assessment, for each reaction a high-recall pool is first constructed via *Multi-Channel Recall*—aggregating
925 reaction-base retrieval, functional-group cues, constraint heuristics, and memory lookup—to produce a Top-5000
926 candidate set spanning Catalyst, Solvent1, Solvent2, Reagent1, and Reagent2. Each model ranks within the
927 same 5k pool and outputs a Top-50 list per head. All models receive identical candidate sets, instructions, and
judgment interfaces, and are not permitted to modify the pool, ensuring that differences reflect discriminative

928 **Algorithm 2** Two-Stage Multi-Tool Collaborative Training

929 **Require:** Datasets $\mathcal{D} = \{(x_i, y_i)\}$; External tools T (`<search>`, `<memory>`, ...);
 930 Instruction I ; SFT epochs E_{sft} ; RL cycles C ; steps per cycle S ; rollouts G ;
 931 GRPO hyper-parameters $(\epsilon, \beta_{\text{KL}})$; temperature τ ; optimizer config.
 932 **Output:** Trained policy π_{θ}^{RL}

933 **Stage I: Chemical Teaching (SFT)** /* cold-start tool-aware policy */

934 1: Initialize backbone model $\pi_{\theta} \leftarrow \text{Qwen3-8B-Instruct}$ ▷ AdamW ($\beta=(0.9, 0.95)$), lr 2×10^{-5} , wd 0.1, batch 128

935 2: **for** $e = 1, \dots, E_{\text{sft}}$ **do** ▷ RL cycles

936 3: Sample minibatch $B \subset \mathcal{D}$ ▷ optimization steps per cycle

937 4: Compute SFT loss $\mathcal{L}_{\text{sft}}(\theta) = -\sum_{(x, y) \in B} \log \pi_{\theta}(y | x)$ ▷ y contains step-wise chain + tool tokens (`<search>`, `<memory>`)

938 5: Update $\theta \leftarrow \theta - \eta \nabla_{\theta} \mathcal{L}_{\text{sft}}(\theta)$

939 6: **end for**

940 7: Freeze SFT checkpoint as reference $\hat{\pi}_{\text{ref}} \leftarrow \text{stopgrad}(\pi_{\theta})$; set $\hat{\pi}_{\theta} \leftarrow \pi_{\theta}$

941 **Stage II: Tool Incentivization (RL with GRPO)** /* align similarity & tool use */

942 1: **for** $c = 1, \dots, C$ **do** ▷ RL cycles

943 2: **for** $s = 1, \dots, S$ **do** ▷ optimization steps per cycle

944 3: Sample a batch $D_b \subset \mathcal{D}$

945 4: **for all** $q \in D_b$ **do**

946 5: $q \leftarrow I \oplus q$

947 6: Sample G rollouts with tools at temperature τ : $\{o_j\}_{j=1}^G \sim \pi_{\theta}(\cdot | q, T)$

948 7: For each o_j , compute reward $R(o_j)$ with hierarchical scheme:
 949 **Format:** if invalid $\Rightarrow R(o_j) \leftarrow -1$
 950 **Similarity:** $\text{Acc}(o_j) \in \{0, 1\}$
 951 **Multi-tool bonus:** $r_M = 0.1$ if (`<search>` & `<memory>`) appear, else 0
 952 **Final:** if format ok, $R(o_j) = \max(\text{Acc}(o_j) + r_M, \text{Acc}(o_j))$

953 8: Compute group-normalized advantages $\{\hat{A}_{j,t}\}$ w.r.t. group baseline
 954 9: Optimize GRPO objective:

955
$$\mathcal{L}_{\text{GRPO}}(\theta) = \frac{1}{G} \sum_{j=1}^G \frac{1}{|o_j|} \sum_{t=1}^{|o_j|} \min(\rho_{j,t} \hat{A}_{j,t}, \text{clip}(\rho_{j,t}, 1-\epsilon, 1+\epsilon) \hat{A}_{j,t}) - \beta_{\text{KL}} \text{D}_{\text{KL}}[\pi_{\theta} \parallel \hat{\pi}_{\text{ref}}]$$

956 10: Update $\theta \leftarrow \theta + \eta \nabla_{\theta} \mathcal{L}_{\text{GRPO}}(\theta)$

957 11: **end for**

958 12: **end for**

959 13: **end for**

960 14: **return** π_{θ}^{RL}

961
 962 ranking and evidence integration rather than retrieval coverage. This protocol mitigates search-space inflation,
 963 reduces hallucination, and provides an evaluation setting consistent with the workflow of the framework.
 964

965 **F EVALUATION PROTOCOL DETAILS**

966 In this section, we provide the formal definition of the structure-aware evaluation metrics used in our experiments.
 967 The Reaction Condition Recommendation (RCR) task requires models to predict appropriate reaction conditions
 968 given reactants and products. We evaluate the quality of predicted condition SMILES strings against ground truth
 969 annotations using molecular fingerprint similarity metrics.

970 **F.1 SMILES CANONICALIZATION AND VALIDITY**

971 Prior to fingerprint calculation, all SMILES strings undergo canonicalization to ensure consistent molecular rep-
 972 resentations. Let \hat{s} be the predicted SMILES and s^* be the ground truth SMILES. The canonicalization procedure
 973 converts input SMILES to a standardized canonical form:

$$s_{\text{canonical}} = \text{Canonicalize}(s_{\text{input}}) \quad (13)$$

974 This process removes representational ambiguity. Consistent with our evaluation constraints, stereochemical infor-
 975 mation is excluded during canonicalization (`isomericSmiles=False`) to focus evaluation on constitutional
 976 structure.

977 The validity metric quantifies the proportion of predictions that correspond to chemically valid molecular struc-
 978 tures:

$$\text{Validity} = \frac{1}{N} \sum_{i=1}^N \mathbb{1}[\text{IsValid}(\hat{s}_i)] \quad (14)$$

986 where $\mathbb{1}[\cdot]$ is the indicator function and $\text{IsValid}(\cdot)$ returns true if the SMILES string can be successfully parsed
 987 into a valid molecular graph by RDKit (version 2023.03 or later). Invalid predictions are assigned a similarity
 988 score of 0 for all fingerprint metrics.
 989

990 F.2 TANIMOTO SIMILARITY

992 All fingerprint-based similarity calculations employ the Tanimoto coefficient (Jaccard index). For two molecular
 993 fingerprints represented as bit vectors \mathbf{A} and \mathbf{B} (corresponding to the predicted molecule M_p and ground truth
 994 molecule M_g), the Tanimoto similarity is defined as:
 995

$$996 T(\mathbf{A}, \mathbf{B}) = \frac{|\mathbf{A} \cap \mathbf{B}|}{|\mathbf{A} \cup \mathbf{B}|} = \frac{c}{a + b - c} \quad (15)$$

998 where a denotes the number of bits set to 1 in \mathbf{A} , b denotes the number of bits set to 1 in \mathbf{B} , and c denotes the
 999 number of bits set to 1 in both fingerprints simultaneously.
 1000

1001 F.3 MOLECULAR FINGERPRINT TYPES

1003 We employ three complementary molecular fingerprint representations to capture different aspects of molecular
 1004 structure:
 1005

1006 **RDK Topological Fingerprint (f_{RDK})**. This is a path-based topological fingerprint. The algorithm enumerates
 1007 all linear paths of length $l \in [1, 7]$ atoms within the molecular graph. Each path is encoded as a hash incorporating
 1008 atomic numbers, bond types, and connectivity. The resulting hash values are mapped to a bit vector of length
 1009 2048. The similarity is computed as:
 1010

$$S_{\text{RDK}}(M_p, M_g) = T(f_{\text{RDK}}(M_p), f_{\text{RDK}}(M_g)) \quad (16)$$

1012 **MACCS Keys Fingerprint (f_{MACCS})**. The MACCS keys fingerprint consists of 166 predefined structural keys,
 1013 each corresponding to specific substructures (e.g., hydroxyl, carbonyl, aromatic rings). For each key k_i ($i \in$
 1014 $[1, 166]$), the bit is set to 1 if the substructure is present. This metric is particularly valuable for comparing
 1015 molecules based on functional group composition:
 1016

$$S_{\text{MACCS}}(M_p, M_g) = T(f_{\text{MACCS}}(M_p), f_{\text{MACCS}}(M_g)) \quad (17)$$

1018 **Morgan Circular Fingerprint (f_{Morgan})**. We employ Morgan fingerprints with a radius parameter of $r = 2$,
 1019 equivalent to ECFP4. This algorithm captures the local chemical environment by iteratively identifying atom
 1020 identifiers and their neighbors. It excels at detecting localized structural differences and functional group modifi-
 1021 cations:
 1022

$$S_{\text{Morgan}}(M_p, M_g) = T(f_{\text{Morgan}}(M_p, r=2), f_{\text{Morgan}}(M_g, r=2)) \quad (18)$$

1024 F.4 AGGREGATE EVALUATION METRICS

1026 To assess the model performance, we utilize the **Fingerprint Tanimoto Score (FTS)**, defined as the validity-
 1027 weighted average of the three fingerprint similarities:
 1028

$$1029 \text{FTS} = \left(\frac{\bar{S}_{\text{RDK}} + \bar{S}_{\text{MACCS}} + \bar{S}_{\text{Morgan}}}{3} \right) \times \text{Validity} \quad (19)$$

1031 where \bar{S}_{type} represents the mean similarity score across all test samples for that specific fingerprint type.
 1032

1033 F.5 TOP- k SIMILARITY

1035 Since our model generates a ranked list of candidate predictions, we also report a Top- k metric. Let $\mathcal{S}(\hat{s}, s^*)$ be
 1036 the pairwise similarity for a single instance, defined as the average of the three fingerprint Tanimoto coefficients
 1037 (assigned as 0 if \hat{s} is invalid).
 1038

1039 For a dataset of N reaction instances, where s_i^* is the ground-truth SMILES and $\hat{S}_{i,k} = \{\hat{s}_{i,1}, \dots, \hat{s}_{i,k}\}$ is the set
 1040 of the top- k predicted SMILES strings:
 1041

$$1042 \text{Score}@k = \frac{1}{N} \sum_{i=1}^N \max_{j \in \{1, \dots, k\}} \mathcal{S}(\hat{s}_{i,j}, s_i^*). \quad (20)$$

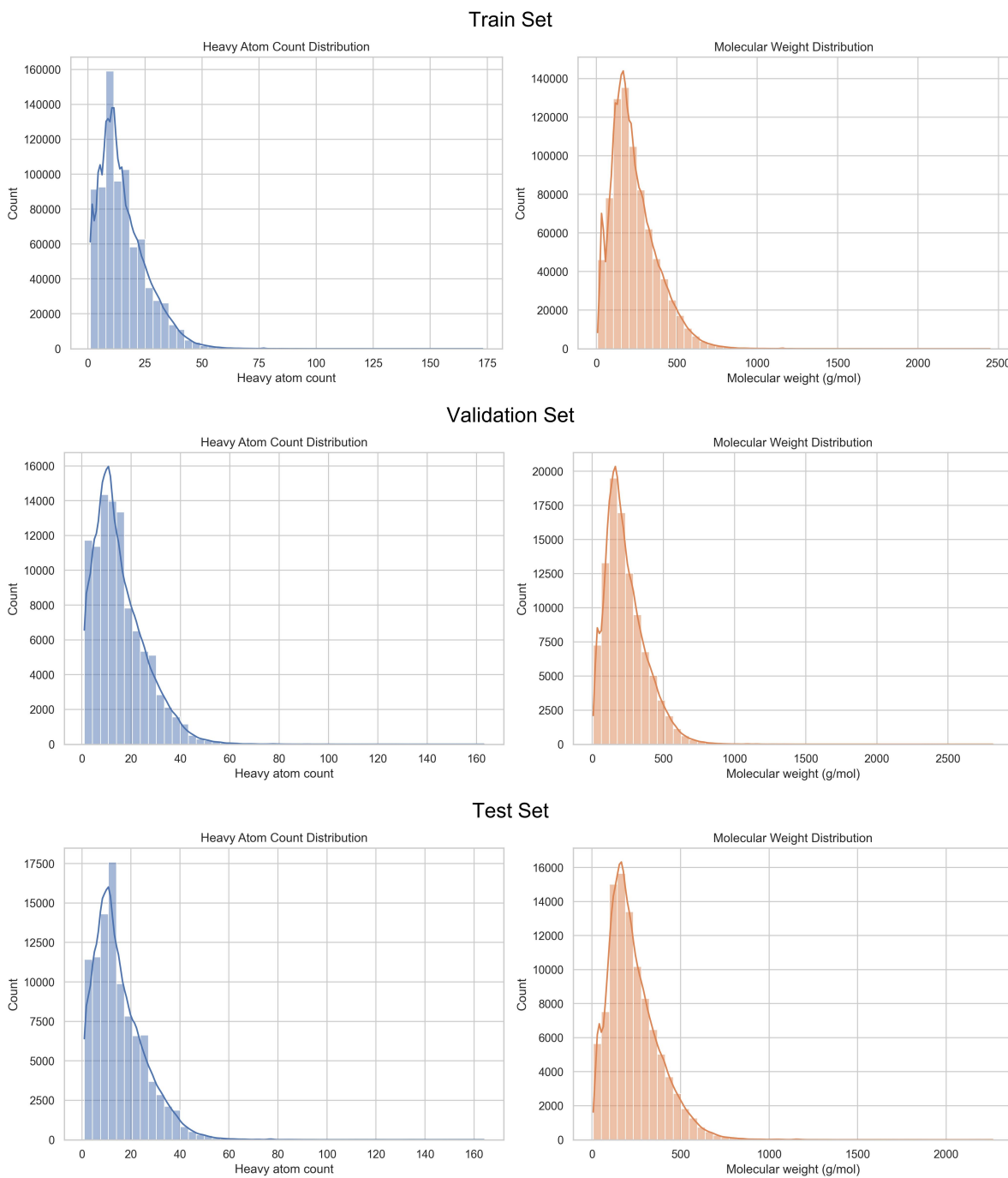


Figure 6: Heavy-atom and molecular-weight distributions for the Train, Validation, and Test sets (top to bottom). Left column: heavy atom count; right column: molecular weight (g/mol).

G DATASET DETAILS

Public Dataset. We use the RCR subset of ChemCoTBench, which contains 90 well-structured samples covering 10 reaction types. For each reaction type, there are 9 examples: 3 focused on catalyst prediction, 3 on reagent prediction, and 3 on solvent prediction. All chemical entities (reactants/products/conditions) are represented in SMILES format to ensure consistency.

Private Dataset. We curate a large-scale private dataset of organic reactions to supplement existing public benchmarks and better represent real-world experimental scenarios. Sourced from the internal database of an anonymous chemical research institution, this dataset is rigorously digitized and structured, comprising 544,591

1102 high-quality entries. Similar in nature to the USPTO-condition dataset, it encompasses a broad spectrum of known
 1103 chemical reactions, reflecting a chemical space.

1104 For data standardization, all chemical entities are represented in SMILES format. Each SMILES string is pro-
 1105 cessed with RDKit to construct a molecular graph; unparseable strings are discarded. For every valid molecule,
 1106 we compute the total atom count, the heavy-atom count (all non-hydrogen atoms), the molecular weight as the
 1107 sum of average atomic masses (g/mol), and the exact mass as the sum of isotopic masses (g/mol). We then an-
 1108alyze and visualize the heavy-atom and molecular-weight distributions for the training, validation, and test sets,
 1109 where the left column shows the heavy-atom counts and the right column shows the molecular weights in g/mol,
 1110 as shown in Figure 6. We frame the task as a reaction condition prediction problem: for each entry, the reactants
 1111 and products serve as the input, while the reaction conditions are defined as the output. To enable fine-grained
 1112 prediction, the output is structured into five distinct roles: catalyst (Catalyst1), solvents (Solvent1, Solvent2), and
 1113 reagents (Reagent1, Reagent2).

1114 Based on this setting, we construct Question-Answer (QA) pairs to facilitate model training. The dataset is ran-
 1115 domly split into training, validation, and test sets with a ratio of 8:1:1. The inclusion of this private dataset
 1116 provides robust supervision signals and allows for the evaluation of model generalization in complex, realistic
 1117 chemical contexts.

1119 H PROMPT TEMPLATES

1120 As shown in **Figure 7** and **Figure 8**, there are prompts for the different agents. Beyond the system-level instruc-
 1121 tion, the prompt is organized into four parts. First, the *Tool Definition* specifies the invocation schema of tools
 1122 together with their expected outputs. Second, the *Interaction Protocol* describes how the agent should interleave
 1123 tool calls with reasoning traces using XML-style tokens, and how the final answer must be returned in a struc-
 1124 tured format. Third, the *Task Prompt* clarifies the objectives. Finally, the *Output Format* enforces a JSON schema
 1125 that standardizes the prediction into fields such as reaction type, main functional groups, by-products, and evi-
 1126 dence. This structured prompt design enables the model to understand tool usage, maintain a consistent reasoning
 1127 procedure, and produce verifiable outputs.

1130 I RESULTS AND DISCUSSIONS

1131 I.1 ADDITIONAL QUANTITATIVE RESULTS

1132 **Top-5 Analysis.** As shown in **Figure 9**, introducing specialized agents consistently improves Top-5 Similarity
 1133 over the $\mathcal{A}_{Gen} + \mathcal{A}_{Full}$ baseline. \mathcal{A}_{Cat} delivers targeted gains on *Catalyst* (+10.1%), aligning with its role
 1134 specialization. \mathcal{A}_{Sol} contributes the most on solvents, improving *Solvent1* and *Solvent2* by +16.4% and +13.4%,
 1135 respectively. \mathcal{A}_{Rea} yields the largest boosts on reagents (e.g., *Reagent1/2* with gains around +18.7% and +13.9%).
 1136 When specialized agents are combined (e.g., +Cat+Sol, +Sol+Rea, +Cat+Rea), the improvements remain additive
 1137 and stable across condition types, and the *Full System* shows the most consistent Top-5 lift across all five heads,
 1138 indicating effective collaboration among role-specialized experts.

1139 **Top-10 Analysis.** As shown in **Figure 10**, the same trend holds for Top-10 Similarity. \mathcal{A}_{Cat} most strongly
 1140 benefits *Catalyst* (+13.1%). \mathcal{A}_{Sol} provides clear gains on *Solvent1/2* (e.g., +10.8% and +13.6%). \mathcal{A}_{Rea} again
 1141 dominates on *Reagent1/2* with sizeable increments (e.g., +17.2% and +9.8%). Pairwise combinations further
 1142 enhance coverage across heads, and the *Full System* achieves the highest Top-10 metrics in a macro sense, evi-
 1143 dencing that multi-agent collaboration scales beyond single-head expertise and produces robust gains under larger
 1144 candidate sets.

1145 I.2 RESULT VISUALIZATION

1146 To better illustrate the performance of our framework, we visualize several representative reactions with both
 1147 predicted and ground-truth conditions. As shown in **Table 5**, the predicted conditions generally align well with
 1148 the ground-truth, especially for solvents and reagents that are strongly correlated with the transformation patterns
 1149 in the reaction. For example, in reactions involving polar functional groups, the model consistently identifies
 1150 appropriate polar solvents such as alcohols or cyclic ethers. Similarly, in palladium-catalyzed cross-coupling
 1151 reactions, the model reliably predicts the use of palladium-based catalysts, demonstrating its ability to capture
 1152 mechanistic priors from training data.

1153 In cases where the predictions slightly deviate from the ground-truth, the model often proposes chemically rea-
 1154 sonable alternatives. For instance, different bases such as potassium carbonate and cesium carbonate are inter-
 1155 changeable under similar conditions, and solvents like ethanol and methanol can play analogous roles. These

1160
 1161
 1162 **# System Prompt**
 1163 You are a chemical assistant for reaction understanding and condition reasoning.
 1164 You receive Reactant and Product SMILES as inputs. You can call THREE tools:
 1165
 1166 **# Tools Definition**
 1167 1) Functional Group Tagger
 1168 - Invocation: <trigger>{ "reactants": [...], "products": [...] }</trigger>
 1169 - Purpose: extract key functional groups (FGs) from given SMILES.
 1170 - Expected result (inside <result> ... </result>):
 1171 {
 1172 "reactants_fg": [...],
 1173 "products_fg": [...],
 1174 "main_fg": ["acyl chloride", "amine", ...]
 1175 }
 1176
 1177 2) Constraint Engine
 1178 - Invocation: <engine>{ "reactants": [...], "products": [...] }</engine>
 1179 - Purpose: perform atom/electron balance and infer by-products.
 1180 - Expected result:
 1181 {
 1182 "balanced": true,
 1183 "by_products": ["HCl", "H2O"],
 1184 }
 1185
 1186 3) Chemical Knowledge Base Search
 1187 - Invocation: <search>{ "query": "..." }</search>
 1188 - Purpose: retrieve evidence related to reaction conditions via keyword search.
 1189 - Expected result:
 1190 {
 1191 "knowledge": [
 1192 {"keyword": "amide formation", "evidence": ["KB:USPTO:..."]}
 1193]
 1194 }
 1195
 1196 **# Interaction Protocol**
 1197 - You may call tools at any time using the XML tokens above.
 1198 - Tool responses are always returned inside <result> ... </result>.
 1199 - Show reasoning process inside <think> ... </think>. For example, <think> This is the reasoning process. </think>
 1200 - Provide only the structured final answer.
 1201
 1202 **# Task**
 1203 Given Reactant and Product SMILES:
 1204 - Use tools to (i) extract Main Functional Groups, (ii) infer By-products, and (iii) retrieve likely Reaction Type
 1205 candidates.
 1206 - Reconcile results to choose the most plausible reaction_type.
 1207 - Output in JSON schema, wrapped inside <answer> ... </answer>.
 1208
 1209 **# Output Format**
 1210 <answer>
 1211 {
 1212 "reaction_type": "string",
 1213 "main_fg": ["string", ...],
 1214 "by_products": ["string", ...],
 1215 "confidence": 0.0,
 1216 "rationale_short": "1-3 sentences summarizing the key cues.",
 1217 "evidence": ["KB:source_or_ID", ...]
 1218 }
 1219 </answer>



Figure 7: Prompt for General Chemist

1212 substitutions highlight the model’s flexibility in generating valid yet diverse solutions, reflecting its capacity to
 1213 generalize beyond exact memorization of training examples.

1214 Overall, the visualization confirms that the framework not only achieves high top- k similarity but also produces
 1215 predictions that are chemically interpretable and robust. The ability to provide both exact matches and plausible al-
 1216 ternatives underscores the potential of our approach for assisting chemists in condition selection and experimental
 1217 design.

1218
1219
1220
1221
1222
1223**# System Prompt**

You are a chemical assistant specialized in reaction condition evaluation.
 Your input consists of:
 - Reactant and Product SMILES,
 - Two candidate sets of reaction conditions (Response 1 and Response 2).

**# Tools Definition**

- 1) Chemical Knowledge Base Search
 - Invocation: <search{ "query": "..." }>/search>
 - Purpose: retrieve knowledge of the reaction type, mechanism, and precedent reaction conditions related to the given SMILES or candidate reagents/solvents.
 - Expected result:


```
{
  "reaction_info": [
    {"keyword": "SNAr methoxylation", "evidence": ["KB:USPTO:..."], "notes": ["NaOMe/MeOH widely used"]},
    {"keyword": "Nucleophilic aromatic substitution", "evidence": ["Reaxys:..."], "notes": ["activated by nitro group"]}
  ]
}
```
- 2) Memory Searching
 - Invocation: <memory{ "memory_type": "main_fg", "by-product" }>/memory>
 - Purpose: retrieve prior memorized knowledge snippets of similar reactions and condition evaluations.
 - Expected result:


```
{
  "content": [
    "main_fg": "Reactant1: methoxy, acyl chloride;Reactant2: -Cl,thiophene ring",
    "by-product": "HCl"
  ]
}
```

Interaction Protocol

- You may call tools at any time using the XML tokens above.
- Tool responses are always returned inside <result> ... </result>.
- Show reasoning process inside <think> ... </think>. For example, <think> This is the reasoning process. </think>
- Evaluations should be concise, evidence-based, and in academic/chemical style.
- If both responses are poor, still select the relatively better one and justify.

Task

- Analyze the chemical transformation (Reactant → Product).
- For each candidate Response, cross-check the catalyst, solvent, reagents against tool outputs (<search> and <memory>).
- Provide a short evaluation of both Response 1 and Response 2.
- Finally, decide which Response is better and explain why concisely.
- Return ONLY the final decision enclosed inside <answer> ... </answer>:

Output Format

```
<answer>
{
  "better_response": "Response 1",
  "response1_eval": "Provides NaOMe in MeOH, directly generating methoxide. Simple, efficient, and canonical for SNAr methoxylation on nitro-activated aryl fluorides.",
  "response2_eval": "Uses K2CO3 in DMSO with MeOH as methoxide source. Feasible but slower, less direct than NaOMe/MeOH.",
  "rationale_short": "SNAr on nitro-aryl fluorides is best driven by a strong methoxide source in MeOH. Literature and memory confirm NaOMe/MeOH is the standard choice."
}
</answer>
```

1269
1270
1271
1272
1273
1274
1275

Figure 8: Prompt for Multi-Agent System

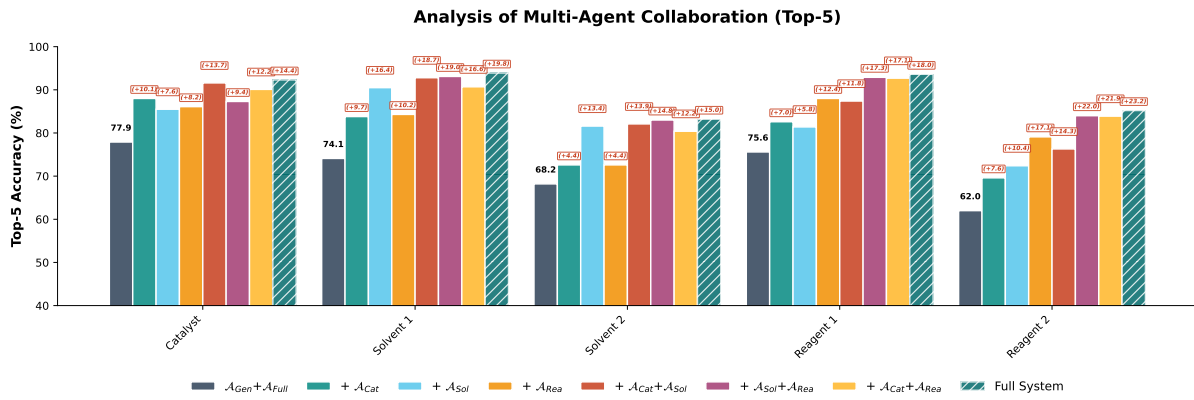


Figure 9: Multi-agent ablation: Top-5 similarity improvements across Catalyst, Solvent1/2, and Reagent1/2 when adding specialized agents on top of $\mathcal{A}_{Gen} + \mathcal{A}_{Full}$.

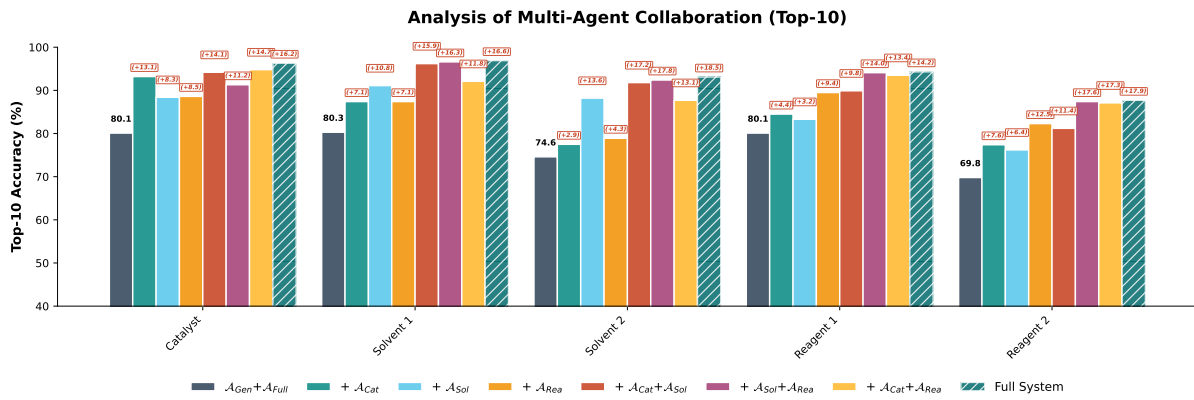


Figure 10: Multi-agent ablation: Top-10 similarity improvements across Catalyst, Solvent1/2, and Reagent1/2 when adding specialized agents on top of $\mathcal{A}_{Gen} + \mathcal{A}_{Full}$.

Table 5: Visualization of several reactions with predicted (blue) vs. ground-truth (red) labels.

	Reactions	Catalyst 1 (Pred / GT)	Solvent 1 (Pred / GT)	Solvent 2 (Pred / GT)	Reagent 1 (Pred / GT)	Reagent 2 (Pred / GT)
1349			AcOH AcOH		Bromine Bromine	
1353			Toluene Toluene		TEA TEA	
1357			EtOH EtOH		Chloride Chloride	NaOH NaOH
1362		Palladium Palladium	MeOH MeOH		THF THF	
1366			THF THF		AIBN AIBN	
1370			MeCN MeCN		K2CO3 K2CO3	
1373		Platinum Platinum	THF THF		TEA TEA	Pyridine Pyridine
1376			Toluene Toluene		K2CO3 Cs2CO3	
1380			EtOH MeOH		H2O H2O	NaOEt NaOMe

1392
1393
1394
1395
1396
1397
1398
1399
1400
1401
1402
1403
1404
1405
1406
1407
1408
1409
1410
1411
1412
1413
1414
1415
1416
1417
1418
1419
1420
1421
1422
1423
1424
1425
1426
1427
1428
1429
1430
1431
1432
1433
1434
1435
1436
1437
1438
1439
1440
1441
1442
1443
1444
1445
1446
1447
1448
1449**Example #1 from Chemical Reasoning Dataset****Question:**

Reactant SMILES: CN1CCN (Nc2ccc (/C=C3/c4ccc (F) cc4OCc4c (F) cccc43) cc2 [N+] (=O) [O-]) CC1.N#CN=C (Oc1cccc1) Oc1cccc1

Product SMILES: CN1CCN (n2/c (=N/C#N) [nH] c3cc (/C=C4/c5ccc (F) cc5OCc5c (F) cccc54) ccc 32) CC1

Select the correct reaction conditions from the following options:

Option A:

```
{ "catalyst1": "N\\\\2=C1\\N(CCCCC1)CCC/2", "solvent1": "CN(C)C=O", "solvent2": "CC#N", "reagent1": "[K+].[K+].[O-]C([O-])=O", "reagent2": " " }
```

Option B:

```
{ "catalyst1": "[Pt]", "solvent1": "C1CCOC1", "solvent2": "", "reagent1": "CCN(CC)CC", "reagent2": "c1ccncc1" }
```

Labeled Answer: Option B

Output of one Agent from ChemMAS

<think> To determine the optimal reaction conditions, I must analyze the structural changes between the reactants and the product. The reactants are a (2-nitrophenyl)hydrazine derivative and diphenyl cyanocarbonimidate. The product is a 2-cyanoiminobenzimidazole fused to the aromatic system. Notably, the reactant contains a nitro group ($-NO_2$) at the *ortho* position, while the product features a benzimidazole ring where the nitrogen from the nitro group has been incorporated into the ring system. This implies a transformation where the nitro group is reduced to an amine to act as a nucleophile for ring closure. I need to verify if the formation of benzimidazoles from *o*-nitrophenylhydrazines and cyanocarbonimidates requires a reductive step or if a simple base-mediated substitution is sufficient. **</think>**

<search>

- The synthesis of 2-amino or 2-cyanoiminobenzimidazoles from (2-nitrophenyl)hydrazine precursors typically involves a reductive cyclization sequence.
- Standard literature (e.g., methods for Noberastine synthesis) indicates that the *ortho*-nitro group must be reduced to an amine ($-NH_2$) to function as the second nitrogen in the imidazole ring.
- Common conditions for this transformation utilize metal catalysts such as Platinum ([Pt]) or Palladium (Pd/C) under hydrogenation conditions to effect the reduction and subsequent cyclization.
- Solvents like THF (Tetrahydrofuran) are commonly used, often with auxiliary bases like Triethylamine or Pyridine to neutralize phenol byproducts.

</search>

<think> Based on the search results, the reaction mechanism proceeds via the initial attack of the hydrazine on the cyanocarbonimidate, followed by the reduction of the nitro group to an amine. This amine then attacks the intermediate to close the ring. Comparing the options: Option A uses K_2CO_3 and DBU (bases) in DMF/MeCN. This is a standard S_NAr condition set but lacks a reducing agent. It cannot convert the NO_2 group to the NH required for the benzimidazole ring. Option B uses Platinum ([Pt]) as a catalyst in THF with amine bases. Platinum is a classic hydrogenation catalyst capable of reducing the nitro group to the amine, facilitating the reductive cyclization confirmed by the literature. Therefore, Option B is the correct set of conditions. **</think>**

<answer> Option B **</answer>**